

<sup>1</sup> Swiss Federal Institute of Technology, Atmospheric and Climate Science, IAC-ETH, Zurich, Switzerland

<sup>2</sup> University of Basel, Institute for Meteorology, Climatology and Remote Sensing, Basel, Switzerland

<sup>3</sup> University of Dresden, Germany

<sup>4</sup> Bulgarian National Institute of Meteorology and Hydrology, Bulgaria

<sup>5</sup> Swiss Federal Institute of Technology, Laboratory of Air and Soil Pollution, LPAS-EPFL, Switzerland

<sup>6</sup> University of Hamburg, Meteorology Department, Germany

<sup>7</sup> Risø National Laboratory, Department for Wind Energy, Denmark

<sup>8</sup> University of Freiburg, Meteorological Institute, Germany

<sup>9</sup> Observatory of Neuchatel, Switzerland

<sup>10</sup> The University of British Columbia, Geography Department, Canada

<sup>11</sup> The National University of Singapore, Geography Department, Singapore

<sup>12</sup> Swiss Federal Office of Meteorology and Climatology, MeteoSwiss, Switzerland

<sup>13</sup> Birmingham University, Geography Department, England

<sup>14</sup> University of Western Ontario, Geography Department, Canada

## BUBBLE – an Urban Boundary Layer Meteorology Project

**M. W. Rotach<sup>1,12</sup>, R. Vogt<sup>2</sup>, C. Bernhofer<sup>3</sup>, E. Batchvarova<sup>4,7</sup>, A. Christen<sup>2</sup>,  
A. Clappier<sup>5</sup>, B. Feddersen<sup>6</sup>, S.-E. Gryning<sup>7</sup>, G. Martucci<sup>9</sup>, H. Mayer<sup>8</sup>,  
V. Mitev<sup>9</sup>, T. R. Oke<sup>10</sup>, E. Parlow<sup>2</sup>, H. Richner<sup>1</sup>, M. Roth<sup>11</sup>, Y.-A. Roulet<sup>5</sup>,  
D. Ruffieux<sup>12</sup>, J. A. Salmond<sup>13</sup>, M. Schatzmann<sup>6</sup>, and J. A. Voogt<sup>14</sup>**

With 24 Figures

Received April 5, 2004; revised August 31, 2004; accepted November 7, 2004

Published online March 31, 2005 © Springer-Verlag 2005

### Summary

The Basel UrBan Boundary Layer Experiment (BUBBLE) was a year-long experimental effort to investigate in detail the boundary layer structure in the City of Basel, Switzerland. At several sites over different surface types (urban, sub-urban and rural reference) towers up to at least twice the main obstacle height provided turbulence observations at many levels. In addition, a Wind Profiler and a Lidar near the city center were profiling the entire lower troposphere. During an intensive observation period (IOP) of one month duration, several sub-studies on street canyon energetics and satellite ground truth, as well as on urban turbulence and profiling (sodar, RASS, tethered balloon) were performed. Also tracer experiments with near-roof-level release and sampling were performed. In parallel to the experimental activities within BUBBLE, a meso-scale numerical atmospheric model, which contains a surface exchange parameterization, especially designed for

urban areas was evaluated and further developed. Finally, the area of the full-scale tracer experiment which also contains several sites of other special projects during the IOP (street canyon energetics, satellite ground truth) is modeled using a very detailed physical scale-model in a wind tunnel. In the present paper details of all these activities are presented together with first results.

### 1. Introduction

Urban boundary layer meteorology has become an issue of increasing concern in recent years. First, air pollution concentrations for most atmospheric pollutants are highest in urban environments and hence air pollution modeling is required when evaluating abatement strategies. However, air pollution models and in particular

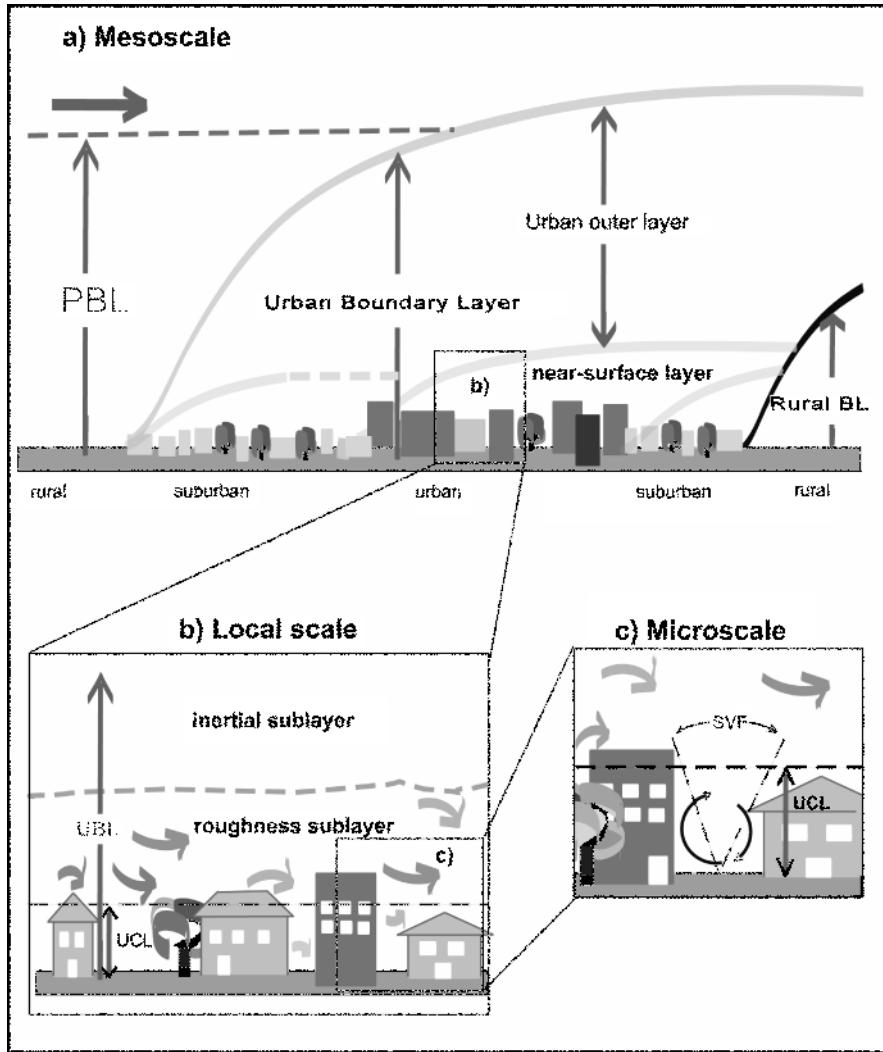


**Fig. 1.** Sketch of the urban boundary layer structure indicating the various (sub)layers and their names (modified after Oke, 1987). In c) SVF stands for sky view factor

their meteorological part, are generally developed for surfaces of lesser roughness and do not take into account the dispersion conditions in the layer near the surface (Rotach, 2001). Second, increasing computer power allows mesoscale meteorological models to be run at higher spatial resolution. For example, the innermost nesting domain of today's weather prediction models has a typical horizontal resolution of 5 to 10 km. Thus more grid points will be truly urban grid points requiring a surface exchange parameterization that takes into account urban surface characteristics and exchange processes. Nevertheless, operational models (and similarly most research models) simply use some urban values for a number of surface-characterizing variables (such as the roughness length or the surface thermal conductivity) without any further modification due to the high roughness elements (Craig and Bornstein, 2002).

The urban boundary layer has a complicated three-dimensional structure making it difficult to comprehensively describe (Rotach et al., 2002). Figure 1 sketches this (idealized) structure and – at the same time – indicates some of the layers and the terminology as used throughout this paper. In the vertical the lowest distinct layer is certainly the *Urban Canopy Layer* (UCL) that ranges from the ground up to roughly the average height of roughness elements (buildings and trees),  $z_H$  (Fig. 1b). It is part of the *roughness sublayer* (RS) the height of which,  $z_*$ , is dependent on the height and density of roughness elements, but for simplicity often expressed as  $z_* = a\bar{z}_H$ , where  $a$  ranges between 2 and 5 (Raupach et al., 1991). Above the RS there is an *inertial sublayer* (IS) that corresponds to the true matching layer over ideal surfaces (Tennekes and Lumely, 1972). Hence under ideal circumstances (stationary conditions, large enough distance to the smooth–

rough transition and the city border, etc.) we may expect Monin-Obukhov Similarity Theory (MOST) to apply within the IS – even if the latter may often be squeezed between the RS and the layers above (Rotach, 1999). Above the IS the urban boundary layer is – except for extensively homogeneous city structures, being the exception rather than the rule – probably to a large extent determined through advective processes (cf. Fig. 1a). Little is known at present whether or not this outer part of the urban boundary layer exhibits characteristics of mixed layer scaling under convective conditions or local scaling under stable stratification. We therefore refer to this layer as to the *outer urban boundary layer* (OUBL) throughout this paper without making a distinction according to stability.

Earlier experiments devoted to investigating the urban boundary layer (UBL) were often either devoted to near-surface characteristics or the general flow and thermodynamic conditions within the OUBL. A notable exception from this rule was the St. Louis study (Clarke et al., 1982) during which both aspects were given equal weight. However, even in this reference study for quite some time, the near-surface turbulence was analyzed in terms of MOST (and deviations thereof) therefore implying a very shallow roughness sublayer. A number of recent near-surface turbulence studies were reviewed by Roth (2000). They reveal, as a common feature, that the turbulent fluxes are not – as opposed to MOST and hence the inertial sublayer – constant with height in the urban roughness sublayer. Secondly, local scaling is found to be a suitable substitute for MOST, once the profile of the turbulent fluxes is known (Rotach, 1993).

Remote sensing observations were sometimes used to investigate the differences between urban and rural boundary layer characteristics (e.g. in the ECLAP study over Paris, Dupont et al., 1997 or earlier by Godovich et al., 1985). Argentini et al. (1999) focused their work on the convective boundary layer structure in Milan under weak wind conditions. In all these studies, only one or two (if at all) surface stations were available. Also, they are typically confined to one or a few episodes. Very little has been attempted so far in order to investigate urban *boundary layer profiles* of meteorological variables most likely due to the mentioned lack of suitable near-surface information.

The present experiment (Basel UrBan Boundary Layer Experiment, BUBBLE) finds itself in a series of recent efforts to combine near-surface and remote sensing instrumentation to obtain a full picture of the UBL. In Marseilles (F) the so-called ESCOMPTE project was part of a larger meteorological effort to investigate the meteorological conditions leading to high ozone concentrations in the complex environment of the Mediterranean coast (Mestayer et al., 2004). URBAN 2000 in Salt Lake City did, in terms of investigating the *urban* boundary layer, focus on pollutant dispersion processes at different scales (Allwine et al., 2002). While the meteorological observations were not particularly dense within the UBL, large efforts were devoted to studying the meteorological structure of the nearby complex terrain as part of VTMX (Durrant et al., 2002).

In this contribution we present details about BUBBLE, the probably longest lasting and one of the spatially most detailed urban boundary layer experiments. It is closely related to COST 715, which is part of the European COST initiative (Joffre, 2002), and devoted to Meteorology Applied to Urban Air Pollution Problems (Fisher et al., 2002). Much of the observational and modeling strategy for this project arises from needs and gaps in our knowledge as identified by the working groups of this COST action (Rotach et al., 2002 for further details). The present paper presents an overview on BUBBLE with selected first results. More in-depth data analyses and modeling results already published are referenced in the respective sections, while further work emanating from BUBBLE will undoubtedly be published at later stages. Section 2 summarizes the observational network and in Section 3 the BUBBLE tracer experiment is described. The next two sections concentrate on numerical (4) and physical (5) modeling efforts that are performed in the context of BUBBLE. An outlook is finally given in Section 6.

## 2. Observational network

### 2.1 Overview

BUBBLE was conducted in the city of Basel in Switzerland (Fig. 2). Basel is a mid-size town (approximately 200,000 inhabitants), surrounded by gentle but non-negligible topography.

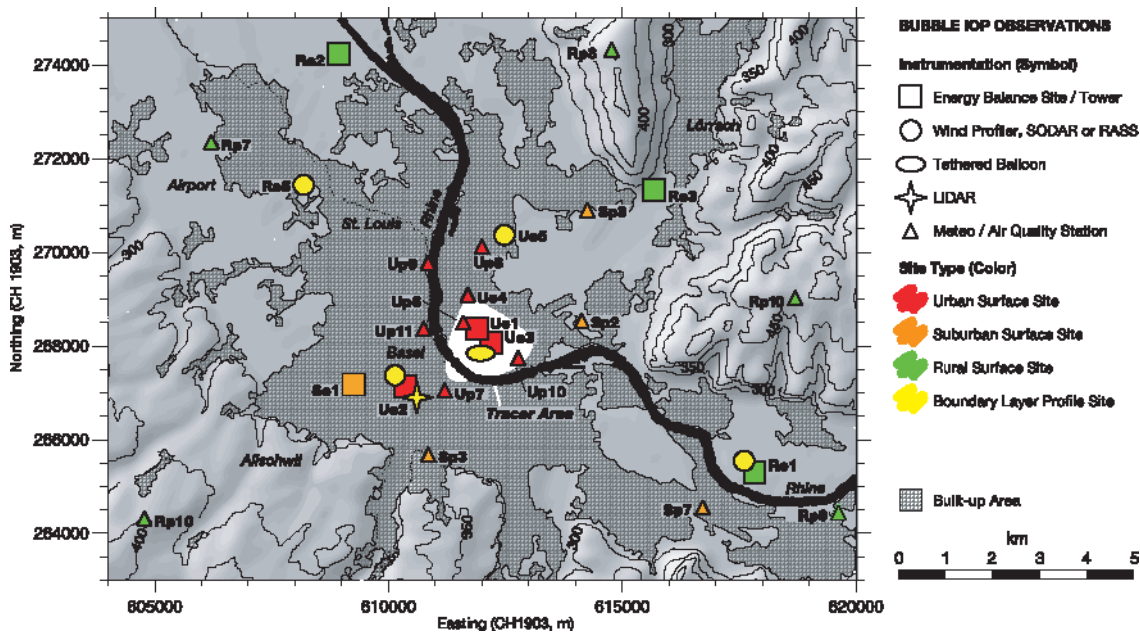


Fig. 2. Overview over the BUBBLE observations in the greater area of the City of Basel. The thick black line denotes the river Rhine. All other symbols explained in the inlet. Note that sites Re4, Sp4, Sp5, Sp6 and Rp6 are outside the shown domain

The general philosophy of BUBBLE was to establish a *long-term* observational network to supplement the already quite dense *permanent* observations (Section 2.2). These long lasting installations (Section 2.3) were scheduled to operate for a *period of one year*. In this spirit, two urban turbulence towers (Section 2.3.1), a Lidar and a Wind Profiler (Section 2.3.2) were operated between summer 2001 and summer 2002. For an intensive observation period (IOP) between June 10 and July 12 2002, additional surface towers were put up in a sub-urban environment and at several rural locations (Section 2.4.1). Also, the turbulence network was largely intensified at one of the urban sites (Section 2.4.3). At the same time the energetics of a street canyon at this urban site were probed in detail (Section 2.4.2). The remote sensing network was extended for the IOP through a RASS system, several sodars, and a tethered balloon at a down town site (2.4.1). Finally, a number of sensors were operated that were specifically designed to provide information for the development and testing of algorithms to retrieve surface information from satellite data (Section 2.4.4).

The BUBBLE dataset involves 30 permanent and experimental surface sites from the greater Basel area. The map in Fig. 2 shows the locations of all surface and ground based remote sensing

measurements. All data are documented and stored in the BUBBLE-database, which includes a web-interface for data selection and download.

## 2.2 Permanent surface sites

The permanent sites are operated by public and private institutions (weather services, local air pollution monitoring authorities, industry). They cover standard meteorological variables measured usually above roof level. Data from the permanent sites are used as background information of the wind and temperature field and are available for the full year of the BUBBLE campaign. Additionally, concentrations of chemical compounds ( $\text{NO}_x$ ,  $\text{O}_3$ , partially  $\text{CO}$ ,  $\text{SO}_2$ ,  $\text{PM}_{10}$ ,  $\text{PM}_{2.5}$ ) are measured at 14 sites.

## 2.3 Long-term observation within BUBBLE

### 2.3.1 Surface sites

**a) Turbulence profile sites.** Two experimental Urban sites (Ue1, Ue2) and an experimental Suburban site (Se1) were designed to determine turbulent momentum, mass and heat exchange. These sites were equipped with towers reaching from street level up to 2 to 2.5 times the mean building height  $z_H$ . At Ue1 a 30 m triangular

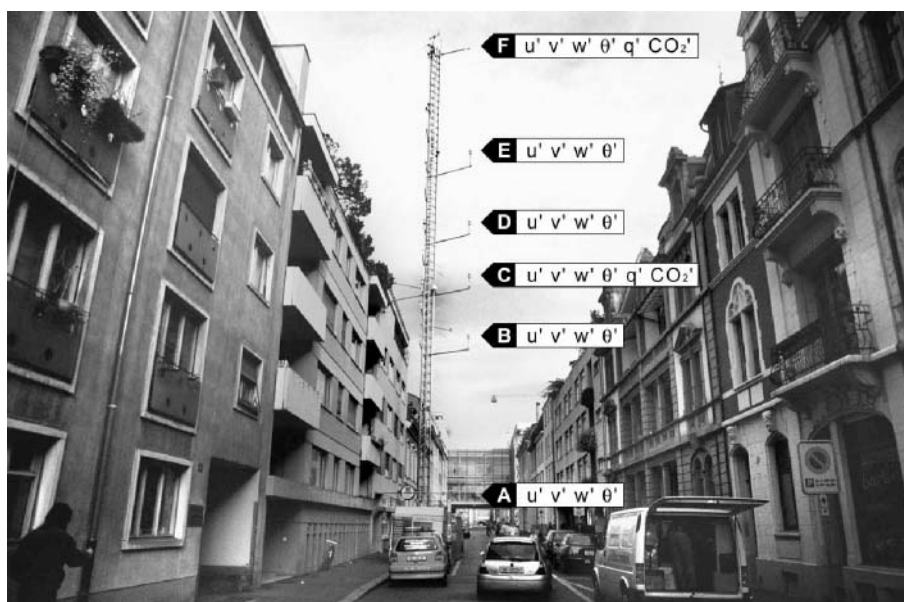


**Fig. 3.** Experimental tower at site Ue1. The arrows indicate the variables measured at the respective levels

lattice tower was placed in a street canyon within a densely built-up part of the city (see Fig. 3). The profile at Ue2 consists of an 18 m tower on top of a building and a profile down into the street canyon, obtained from 5 m-booms on the wall. The suburban site Se1 provides turbulence information from instruments on a hydraulic tower, set up in a vegetated suburban backyard surrounded by two story single and row-houses. All three towers supported simultaneously measured profiles of 3D-ultrasonic anemometer-thermometers with a vertical resolution of 6 instruments at Ue1 and Ue2 and 3 instruments at Se1. The two urban tower sites Ue1 and Ue2 were both operated over nearly one year from fall 2001 until summer 2002, while Se1 was operating only during the IOP. Raw data (20 Hz) of 3D-wind, temperature and water vapor were stored over the whole campaign, resulting in approximately 100 GB. Data were sampled quasi synchronized which allows the investigation of spatial cross-correlations and the vertical interaction of coherent structures. Additionally, the sites were equipped with profiles of temperature/humidity sensors, cup anemometers, full radiation instrumentation and at Ue1 with a vertical profile of  $\text{CO}_2/\text{H}_2\text{O}$  concentrations, sampled with a closed path gas-multiplexer system that sucked sequentially air from 10 tower levels (see Table 1 for details).

The BUBBLE dataset will be exploited in order to verify local scaling approaches (Christen and

Rotach, 2004) and improve parameterizations for higher moments and turbulent fluxes (Rotach et al., 2003b; Christen et al., 2003a). Detailed long-term profiles arise from these sites, as illustrated in Fig. 4. These ensemble profiles represent characteristics for the whole observation period including different wind directions and stabilities. Similar to plant canopies the wind profiles show an inflection point around  $z_H$  and a second maximum inside the canyon. Highest values for  $C_D$  were observed at both canyons between  $0.8z_H$  and  $z_H$ , where the strong drag is caused on one hand by the large and exposed roof areas and on the other hand by the interaction with the canyon and backyard air masses. It is not surprising, that both the wind and  $C_D$  profiles around roof level vary highly dependent on wind direction of the approaching flow relative to the canyon: At roof-level the flow perpendicular to the canyon leads to a horizontal drag which is twice the one observed under along canyon flows.

**b) Energy balance network.** Eight energy balance sites were operated simultaneously in and around the city of Basel during the IOP (see Fig. 2, Table 1). The experimental energy balance sites were all located in flat areas and the locations were chosen with fairly homogeneous surface properties in the prevailing wind directions. The eight sites provide all continuously measured standard meteorological parameters, turbulent fluxes, profiles of temperature,

**Table 1.** BUBBLE sites and characteristics. Symbols for their names are constructed from ‘U’ (urban), ‘S’ (suburban) or ‘R’ (rural), followed by a letter ‘e’ (experimental as opposed to permanent) and an identifying number. Morphometric data from a high-resolution 3d-model of the city (© GVA Basel Stadt)

Code Site Name	Landuse Location	Lat/Lon (WGS-84) Height (a.s.l.)	Surface characteristics <sup>1</sup>	Profiles/Slow Metro <sup>2</sup> [No of Levels]	Turbulence [No of Levels]	Radiation <sup>3</sup> [No of Instr.]	Remote Sensing
Ue1 Basel-Sperrstrasse	Urban Street canyon, mainly residential 3 to 4 storey	47° 33' 57.2" N 7° 35' 48.8" E 255 m	$z_H = 14.6$ m, $\sigma_{z_H} = 6.9$ m $\lambda_P = 0.54$ , $\lambda_F = 0.37$ $\lambda_C = 1.92$ , $\lambda_S = 1$ , $\alpha = 11.0\%$	WV [12], WD, T [7], H [7], CO <sub>2</sub> /H <sub>2</sub> O [10], NO <sub>x</sub> [6], P, S/cT [21]	Sonic ( $u', v', w', t'$ ) [8], $q'$ [3] CO <sub>2</sub> ' [2], Scintillometer [2] (see Table 4)	$R_{sd}$ [3], $R_{sur}$ [2], $R_{ld}$ [5], $R_{lu}$ [3], Thermal Scanner [2], IRT [11].	
Ue2 Basel-Spallenring	Urban Vegetated street canyon residential/commercial 3 to 5 storey	47° 33' 17.6" N 7° 34' 34.6" E 278 m	$z_H = 12.5$ m, $\sigma_{z_H} = 5.4$ m $\lambda_P = 0.37$ , $\lambda_F = 0.31$ $\lambda_C = 1.75$ , $\lambda_S = 1.8$ , $\alpha = 11.2\%$	WV, WD, T [7], H [7], P, N, NO <sub>x</sub>	Sonic ( $u', v', w', t'$ ) [6], $q'$	$R_{sd}$ , $R_{sur}$ , $R_{ld}$ , $R_{lu}$	LIDAR, Wind Profiler
Ue3 Basel-Messe	Urban Parking lot on top of 26 m building	47° 33' 47.6" N 7° 36' 2.6" E 255 m	$z_H = 18.8$ m, $\sigma_{z_H} = 6.3$ m $\lambda_P = 0.41$ , $\lambda_F = 0.25$ , $\lambda_C = 1.64$ , $\alpha = 32.7\%$	T, H, SHF [2]	Sonic ( $u', v', w', t'$ ), $q'$	$R_{sd}$ , $R_{sur}$ , $R_{ld}$ , $R_{lu}$	Tethered Ballon
Ue5 Basel-Kleinmüningen	Industrial Railway track area	47° 35' 5.5" N 7° 36' 15.6" E 265 m			Sonic ( $u', v', w', t'$ )		SODAR MODOS, RASS (Metek GmbH)
Se1 Allschwil	Suburban Vegetated backyard, residential single and row houses, 2–3 storey	47° 33' 19.0" N 7° 33' 41.5" E 277 m	$z_H = 7.5$ m $\lambda_P = 0.28$ $\alpha = 13.2\%$	T, H	Sonic ( $u', v', w', t'$ ) [3], $q'$	$R_{sd}$ , $R_{sur}$ , $R_{ld}$ , $R_{lu}$	
Re1 Grenzach	Rural Grassland	47° 32' 12.0" N 7° 40' 31.5" E 265 m	$\alpha = 22.2\%$	WV, WD, T, H, SHF [3], ST [4], N	Sonic ( $u', v', w', t'$ )	$R_{sd}$ , $R_{sur}$ , $R_{ld}$ , $R_{lu}$ , $R_{net}$	SODAR FAS64
Re2 Village Neuf	Rural Bare Soil	47° 37' 7.6" N 7° 33' 27.1" E 240 m	$\alpha = 19.2\%$	WV [2], WD, T [3], H [3], SHF [3], ST [4], P	Sonic ( $u', v', w', t'$ )	$R_{sd}$ [2], $R_{sur}$ [2], $R_{ld}$ , $R_{lu}$ , $R_{net}$	
Re3 Basel-Lange Erlen	Rural Grassland	47° 35' 32.3" N 7° 38' 56.9" E 275 m	$\alpha = 21.4\%$	WV [3], WD, T [4], H [4], SHF [3], ST [4], N		$R_{sd}$ , $R_{sur}$ , $R_{ld}$ , $R_{lu}$	
Re4 Gempen	Rural Agriculture	47° 28' 20.0" N 7° 40' 21.4" E 710 m	$\alpha = 18.6\%$	WV [4], WD, T [4], H [4], SHF [3], ST [4], N		$R_{sd}$ , $R_{sur}$ , $R_{ld}$ , $R_{lu}$	
Re5 St. Louis	Rural/Industrial Grassland/gravel pit	47° 35' 38.9" N 7° 32' 46.7" E 250 m					SODAR FAS64

<sup>1</sup>  $z_{HF}$ : average building height,  $\sigma_{z_H}$ : standard deviation of building height,  $\lambda_P$ : plan aspect ratio,  $\lambda_F$ : frontal aspect ratio (mean of all wind directions),  $\lambda_C$ : complete aspect ratio,  $\lambda_S$ : Local street canyon aspect ratio at tower base,  $\alpha$ : shortwave albedo. Morphometric parameters of the sites Ue1, Ue2 and Ue3 are calculated for a 250 m circle around the sites based on 1 m raster data of 3d digital building model. Vegetation is not included. Morphometric parameters are calculated according Grimmond and Oke (1999)

<sup>2</sup> WV: wind velocity (cup/propeller), WD: wind direction (vane), T: air temperature, H: humidity, P: pressure, N: precipitation, SHF: storage heat flux, ST: soil temperature, S/cT: surface thermocouples

<sup>3</sup>  $R_{sd}$ : shortwave downward radiation,  $R_{sur}$ : shortwave upward,  $R_{ld}$ : longwave downward,  $R_{lu}$ : longwave upward,  $R_{net}$ : additional net radiometer, IRT: infrared thermometers

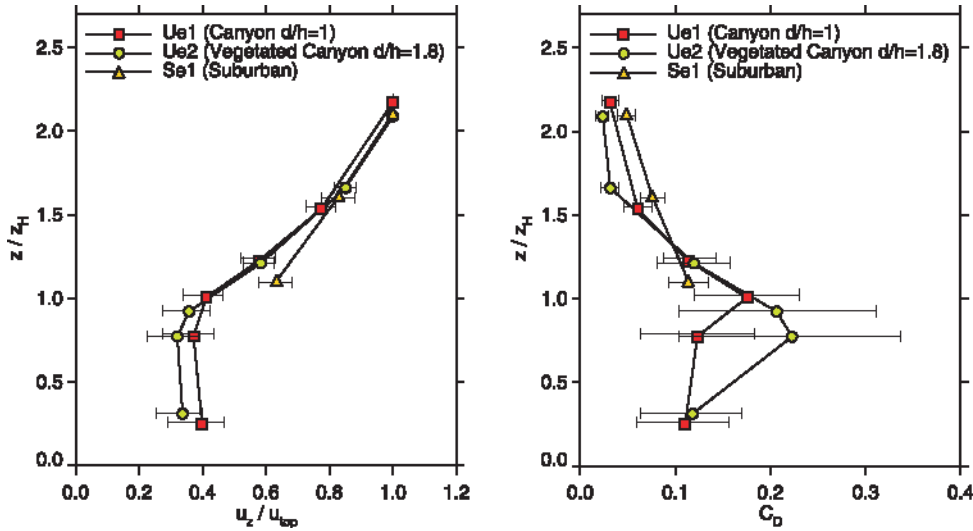


Fig. 4. Mean annual profiles at three (sub)urban sites of, left: horizontal mean wind scaled by wind speed at tower top ( $z/z_H \approx 2$ ), right: local drag coefficient  $C_D = (u_{xz}/u_z)^2$ . The horizontal error bars represent the run-to-run variability (25 and 75% quartiles, respectively). Symbols as indicated in the inlets. The subscript  $z$  denotes here the local height where the variable is evaluated

humidity and wind, radiation and partially storage heat flux measurements. The four components of the radiation balance  $Q^*$  were measured explicitly at all sites. Sensible and latent heat fluxes are directly derived from eddy covariance measurements of 3D-ultrasonic anemometer-thermometers coupled with humidity fluctuation measurements (CSI Krypton KH2O or Li-7500, except at Re3 and Re4). At the built-up sites the eddy covariance measurements were mounted on towers at a height between two and three times the mean building height  $z_H$ . The simultaneous operation of this experimental network allows detailed investigation of the radiative properties and the partitioning of turbulent fluxes over different urban and rural surfaces under the same synoptic forcing with direct rural–urban comparison possibilities.

In Fig. 5 a sample clear-sky day (June 26, 2002) is presented: The higher short-wave radiative energy gain of the city – an effect of the lower albedo at the urban sites – is mostly counterbalanced by its higher long-wave emission, resulting in a more or less equal net radiation  $Q^*$  at all sites. Since latent heat fluxes  $Q_E$  are mainly driven by the fraction of vegetation, it is not surprising that the city center (Ue1, Ue2) with its low vegetation fraction between 15 and 30% shows smaller values. With increasing vegetation towards suburban (Se1) and rural surfaces

(Re1),  $Q_E$  becomes more and more important. Oppositely, the daytime turbulent flux of sensible heat  $Q_H$  is increasing with higher building density, but not so strongly since the storage heat flux is also increased in built-up areas. At all urban sites and at the suburban site, the storage heat flux  $G$  was determined as residual term. At the urban sites, the daytime storage uptake is two to three times higher than at the rural sites. During night, the release of this stored energy at the built-up sites is even higher than the radiative loss. The excess energy is put into the nocturnal upward directed turbulent fluxes (Christen et al., 2003b). A closer look to the temperatures at all sites illustrates, that the nocturnal release of storage heat results in a nocturnal urban heat island. On the other hand, the huge daytime uptake of heat by the building materials produces an urban cold island (see Fig. 5, top panel).

### 2.3.2 Long-term remote sensing observations

**a) Wind profiler.** The Swiss Federal Office for Meteorology and Climatology, MeteoSwiss, operated a low-tropospheric UHF 1290 MHz LAP3000 wind profiler (Ecklund et al., 1988; Ruffieux, 1999). A 15 month-long (1 July, 2001–2 October, 2002) dataset of both wind speed and wind direction semi-hourly profiles was collected next to downtown Basel (at site

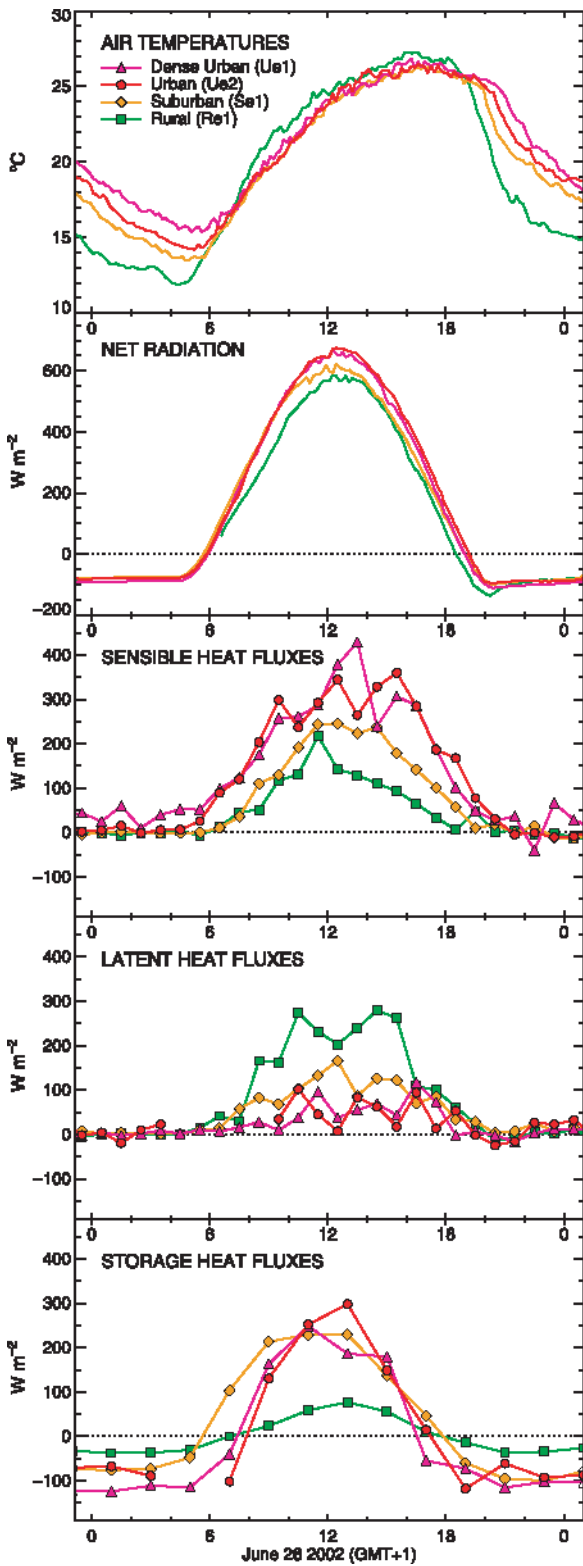


Fig. 5. Diurnal cycles of air temperature, net radiation, sensible, latent and storage heat fluxes for June 26 2002 at sites Ue1, Ue2, Se1 and Re1 (Same day as in Figs. 8, 16–18)

Table 2. Operation modes of the wind profiler during BUBBLE

	High mode	Low mode
First gate	289 (m agl)	145 (m agl)
Last gate	4336 (m agl)	1272 (m agl)
Vertical resolution	202 (m)	43 (m)
Consensus time	30 minutes	30 minutes

Ue2). The system was located within an urban backyard surrounded by buildings.

The operation modes are shown in Table 2 and the parameters calculated at each height are: wind components ( $u$ ,  $v$ ,  $w$ ), wind speed and direction, and signal-to-noise ratio. All raw spectra were recorded and stored. Calculation of consensus was performed using a simple peak algorithm (Weber et al., 1993). An automatic quality control was used in real time and a supplementary quality check was manually performed for a period including the IOP (1–21 July, 2002). The overall data availability in function of height and for the two running modes is shown in Fig. 6. Note that possible bird contamination (Wilczack et al., 1995) can pass through the first level of quality control (seen mainly between 1600 and 2600 m asl in Fig. 6), but are filtered with the second manual quality control.

The wind profiler data can be used to retrieve information on the vertical motions and the mixing depth. By reprocessing the raw data, it is possible to improve the temporal resolution of

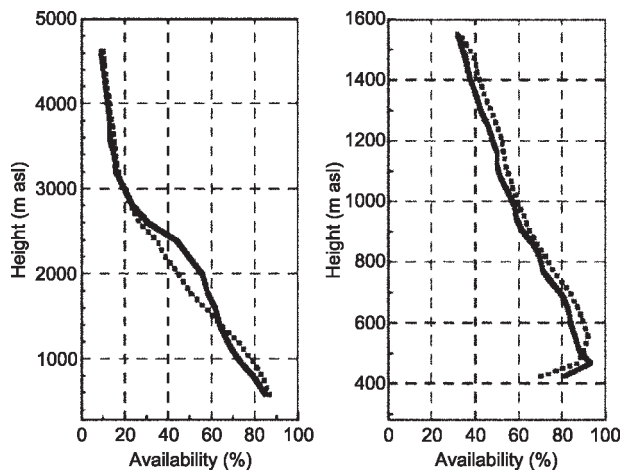
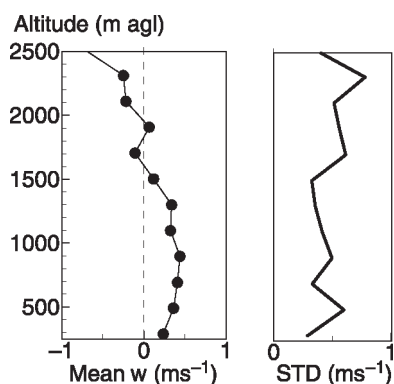


Fig. 6. Overall wind profiler data availability (solid lines) as well as data availability during the IOP (dashed line) for the high mode (left panel) and the low mode (right panel)



**Fig. 7.** Evening time (19 h–01 h CET) mean and standard deviation (STD) profiles of vertical velocity, 17/18 May, 2002, calculated from reprocessed wind profiler 10-min consensus data

the time series. Application of this method to one clear day showed interesting temporal evolution of the vertical motions profiles during the course of one clear day (Ruffieux et al., 2002) with significant ( $>1 \text{ ms}^{-1}$ ) vertical wind in the evening from ground up to 1500 m agl (Fig. 7). By analyzing the height of the maximum signal-to-noise ratio (White, 1993), it will be possible to describe the various steps of the PBL evolution above the city of Basel for specified cases.

**b) Lidar.** A lidar was operated during BUBBLE to detect the relative variation of the atmospheric aerosol vertical profile within the urban planetary boundary layer and the lower troposphere. The lidar is a single wavelength, backscatter-depolarisation instrument, realized at the Observatory of Neuchâtel (Switzerland). During BUBBLE the lidar was operated at roof level at site Ue2. Its operation in Basel was automatic

and remotely controlled from the premises of the Observatory of Neuchâtel (Martucci et al., 2003). The measurement characteristics of the lidar are summarized in Table 3.

As the aerosol is a tracer, the Aerosol Mixed Layer height (AML height) obtained from the lidar signal may be considered a substitute for the PBL height. From the lidar signal there may be obtained also the altitudes and the aerosol backscatter ratio of other aerosol layers and sub-visible clouds, as well as cloud-base height of opaque clouds. Lidar data were continuously recorded between October 2001 and July 2002. The AML height was determined from the range-corrected signal in the following way: Select the most pronounced local minimum of the derivative of the logarithm of the signal, which is closest to the surface. As an additional condition continuity in time is enforced (Frioud et al., 2003; Menut et al., 1999).

Figure 8 presents the range-corrected lidar signal (upper panel) and its derivative (lower panel) for 24 hours starting 14:00 CET (13:00 UTC) on 26 June 2002. This time-height cross-section presents a complicated PBL development with a step-wise AML, on which we also distinguish superimposed accumulation layers. There is clearly a well-mixed layer (its height marked  $x$ ), with a pointed diurnal cycle. Various stages of PBL development are visible from this example: the convective growth of the PBL top in the morning of June 27, the decay in the late evening of June 26, a complex residual layer during the night. For some periods more than one altitude with local minima of the lidar signal derivative

**Table 3.** Specifications of the lidar instrument as operated during BUBBLE

Laser	Wavelength	532 nm
	Average Output power	18–20 mW
	Pulse repetition rate (prf)	5–6 kHz
Receiver	Effective aperture	100 mm $\emptyset$
	Range of full overlap	180 m
Detection and data acquisition	Detection type	Photon counting, two independent channels ('p' and 's' polarizations)
	Range resolution	10 m
	Technical Detection range	Up to approx. 19 km
	Number of laser pulses for a single measurement	Adjustable, 100 to 2,000,000 pulses

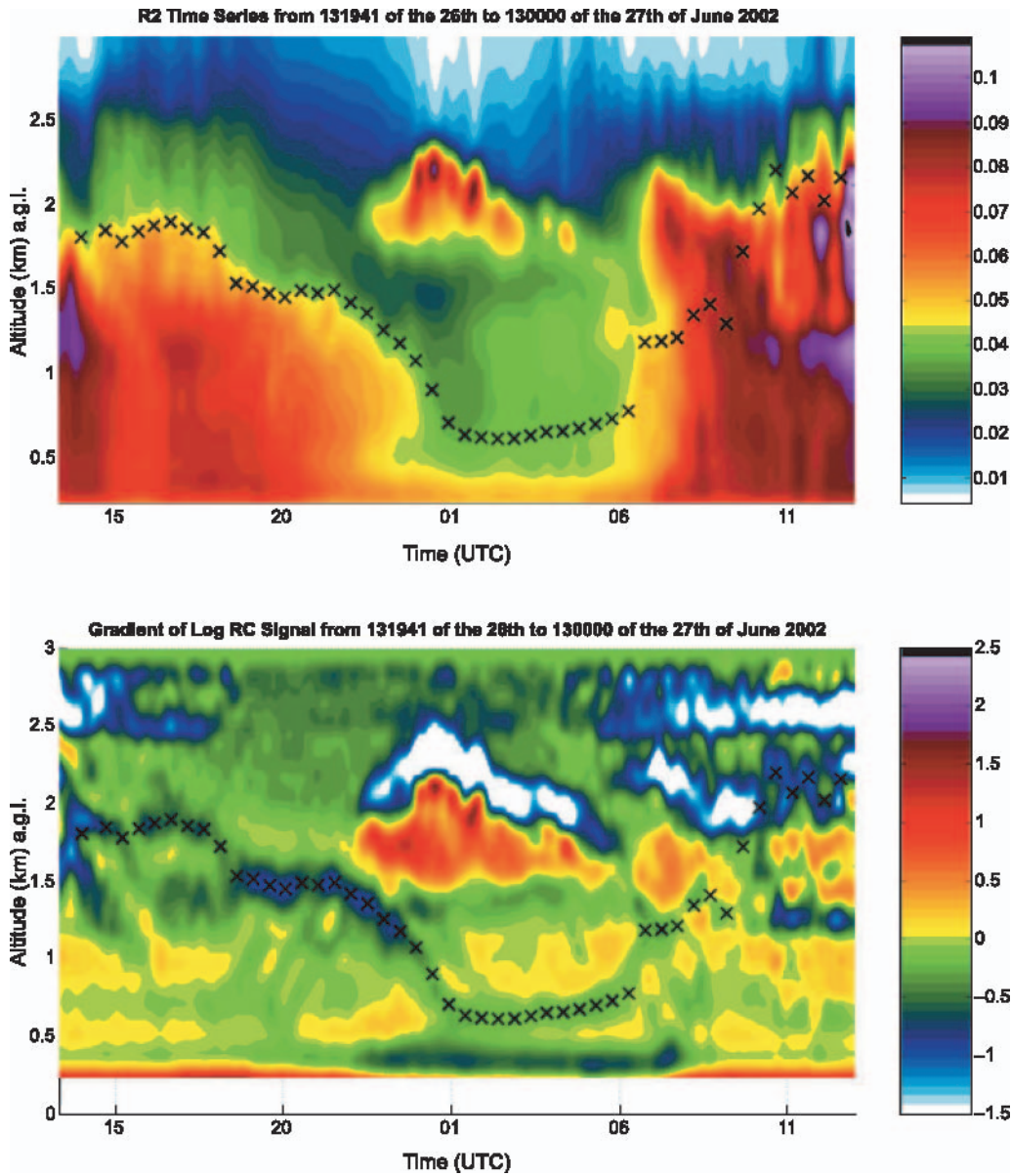


**Fig. 8.** Time-height cross-section of the range-corrected lidar signal (upper panel) and log-derivative of the range-corrected lidar signal (lower panel) from 1300 UTC (14:00 CET) on 26 June 2002 to 1300 UTC (14:00 CET) on 27 June 2002. The color code is proportional to the aerosol load and the magnitude of the derivative, respectively. Crosses represent the objectively determined height of the Aerosol Mixed Layer (see text)

may be identified. These are likely due to processes of accumulation and mixing during the convective development of the PBL. During the night, associated with the residual layer there is a detached aerosol layer at the height of the daytime AML top. For such situations the additional criterion of time-continuity to determine the AML height becomes critical. This illustrates some of the difficulties inherent in the determination of the AML top. It is interesting to note that

there is another local minimum in the lidar signal derivative at 2.0–2.5 km, i.e., above the identified AML top with its clear diurnal cycle. While during the night this height seems to correspond to a residual layer height, the situation is more complicated during the day. Apparently, a layer above the mixed layer, still having considerable aerosol concentration is present in these situations as was noticed by other authors in earlier studies (Arritt and Young, 1990).

## 2.4 IOP activities

### 2.4.1 Additional remote sensing network

Two Doppler sodar systems (MFAS, Scintec, Germany) were operated from May to July 2002 (thus spanning the IOP) outside the urban area, in order to monitor the up-and downwind conditions of the wind field (sites Re5 and Re1). Both sodars were operated in a multi-frequency mode. This limited the data availability and the reliability of the measurements to heights below 300 m. One system was therefore changed to single frequency pulse towards the end of the campaign and then had a data availability >90% up to 480 m.

As part of two of the tracer release experiments (Section 3), tethered balloon soundings were carried out in the center of the city (Ue3). During the first experiment the balloon escaped halfway through but the second experiment was successful and a 24 h period of profiles of wind speed, wind direction, temperature and humidity was sampled. Figure 9 shows the build-up of the nocturnal inversion over the urban area, which goes together with a change in wind direction. The inversion grows to a 200–300 m thick layer agl and is supported by the developing nocturnal

low-level jet. Note that the near-surface turbulent heat flux remains positive at all levels at site Ue1 (not shown, but cf. Fig. 5 for a similar night). Clearly, the profile in Fig. 9 may not have sufficient vertical resolution, especially at the lowest levels, to directly assess the local flux-gradient relation. However, this observation shows that a positive near-surface turbulent heat flux may not necessarily imply an unstable static stability (as sometimes concluded) for the entire lower UBL. Towards the morning the flow in the whole layer up to 1000 m has switched to east–southeast, where the cold air drainage from the Swiss Midlands and the High Rhine Valley comes from. Subsequent warming and convection finally breaks up the inversion.

One Doppler-sodar/RASS system (MODOS and 1290 MHz RASS MERASS, METEK, Germany) was operated in northern part of the urban area of Basel (site Ue5) for the period June 6 to July 9 2002 (i.e. roughly the IOP). Profiles of wind, temperature and some turbulence variables were measured between 40 m and 500 m with a vertical resolution of 20 m. Figure 10 shows a comparison of the profiles of temperature, humidity and wind speed from the various remote sensing

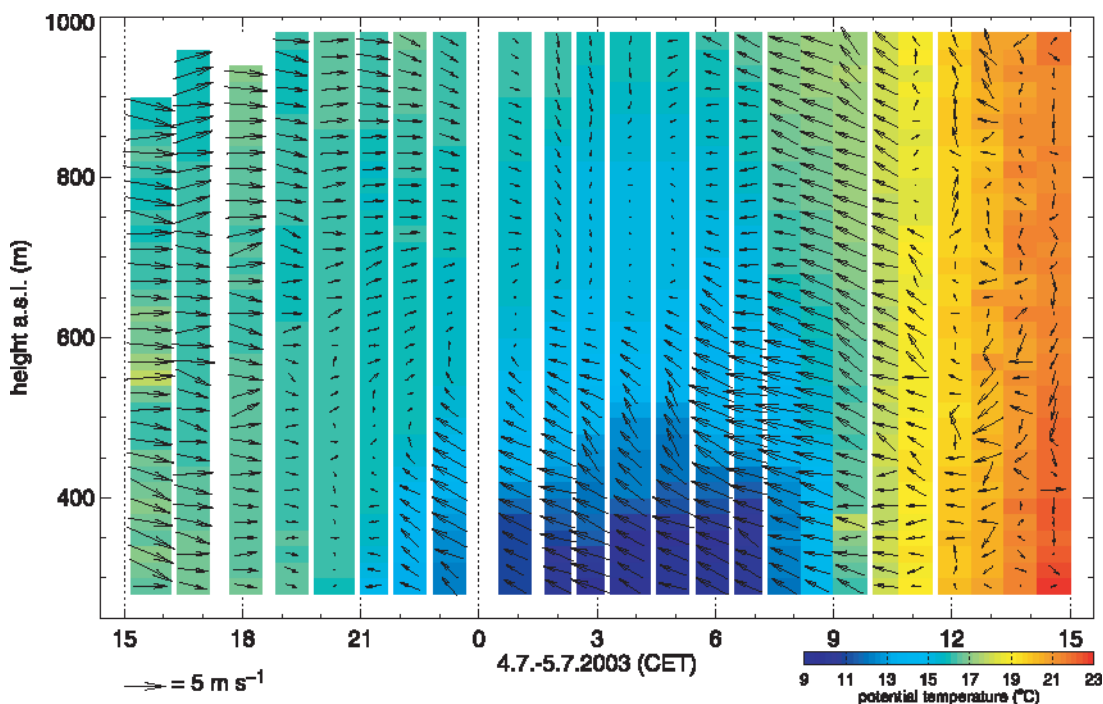


**Fig. 9.** Tethered balloon soundings in the city center (site Ue3). Each color column refers to one ascent/decent, which are averaged into layers with 20 m resolution. Potential air temperature is displayed as color code, wind speed and direction (in the horizontal plane) as arrows

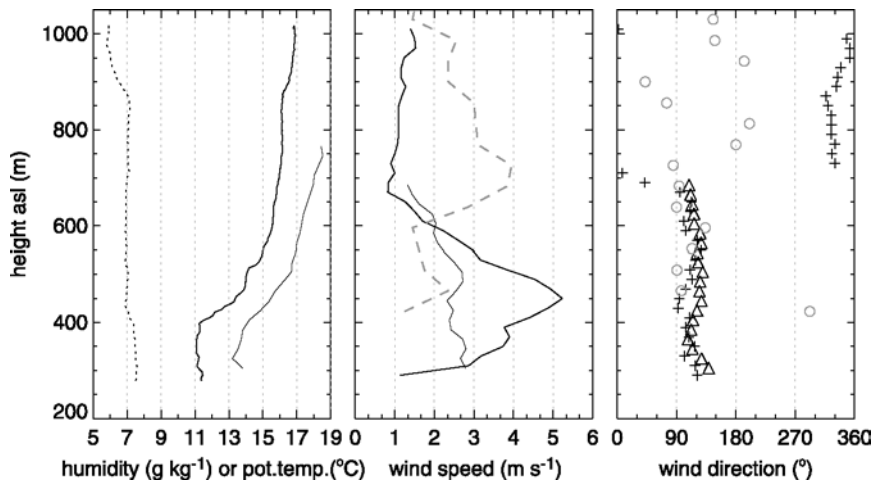


**Fig. 10.** Comparison of temperature and specific humidity (left panel), wind speed (middle panel) and wind direction (right panel) on July 5 2002. Data from the wind profiler at site Ue2 (dashed line, circles), tethered balloon at site Ue3 (bold lines, dotted line (humidity), +) and RASS at site Ue5 (thin line, triangles)

instruments employed within City of Basel during the IOP. Although the RASS and the tethered balloon exhibit an offset of about 2 K, the *profiles* look highly comparable thus suggesting that the temperature field may be quite homogeneous (cf. the horizontal distance of sites Ue3 and Ue5 in Fig. 2). An excellent agreement between all the three systems is found for the wind direction at least up to about 700 m. This corresponds to the establishment of a thermal wind due to the nearby topography, which is quite uniform over large parts of the city. Wind speed finally exhibits the largest site-to-site (or maybe instrument-to-instrument) differences. At Ue2 an elevated maximum is observed at or near the boundary layer height. On the other hand the balloon soundings at site Ue3 suggest a low-level jet clearly within the stable nocturnal boundary layer and the RASS profile at Ue5 yields little vertical variability. Systematic evaluation of similar cases will have to show to what extent these differences reflect spatial inhomogeneity in the wind field or measurement uncertainties of the various systems used.

#### 2.4.2 Street canyon energetics

The dense array of long-term measurement systems at the Ue1 canyon site (Sperrstrasse canyon, or SC in the following; Fig. 11) as summarized in Table 1 formed a solid base to gain understanding of the one-dimensional exchanges and microclimatic responses of this densely developed central urban neighborhood. During the IOP aspects of the two- and three-dimensional characteristics of the canyon system were also investigated. These included:

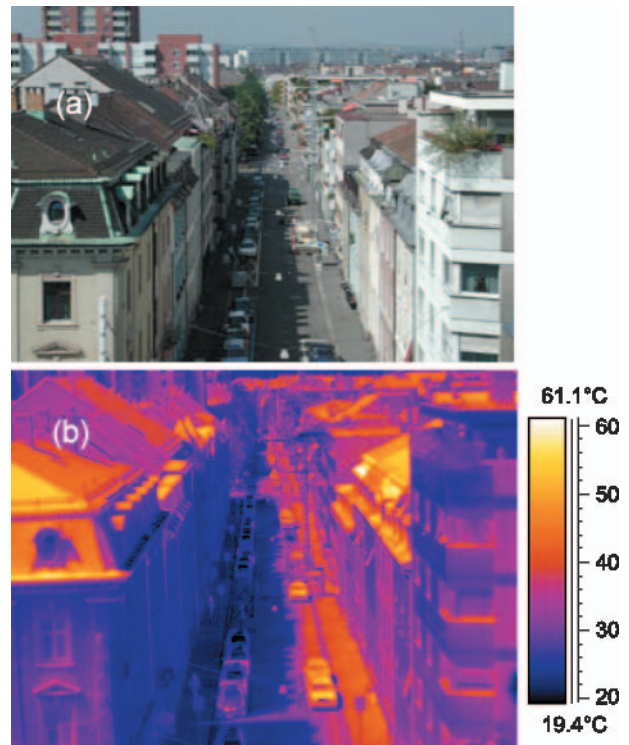


**Fig. 11.** a) Photograph of the urban canyon at site Ue1 looking to the west. The tower is mounted on the north side of the street canyon at about mid-block, this is also the location of the cross-sectional array. b) Thermal image of site Ue1 taken at 11:20 CET with a FLIR SC500 thermal scanner

- Detailed monitoring of the surface temperature responses of the canyon facets (walls and floor) to the dynamic diurnal sun-shade environment;
- The relative contribution of heat fluxes to and from the canyon volume versus those of the nearby roofs to the spatially-integrated fluxes sensed above the roughness sub-layer;

- The air temperature change inside the canyon air volume, and the relative contributions to it made by radiative versus turbulent heat flux convergence/divergence.

To accomplish these objectives the canyon instrument array was supplemented by additional thermal and flux sensors (Fig. 12 and Table 4). Most attention was paid to the perimeter of a two-dimensional cross-section across the canyon near the long-term tower. The surface thermal characteristics of the SC facets were monitored

using a range of *in-situ* and remote sensors. They provided data that varied in spatial content from point measurements to averages of canyon upwelling infrared radiation from hemispherical-view instruments. Altogether, 41 sensors were deployed. The measurements provide information concerning both micro-scale spatial patterns of canyon surface and air temperature and their temporal evolution. A combination of direct and remote measurement systems provided a unique view of UCL level thermal characteristics, not

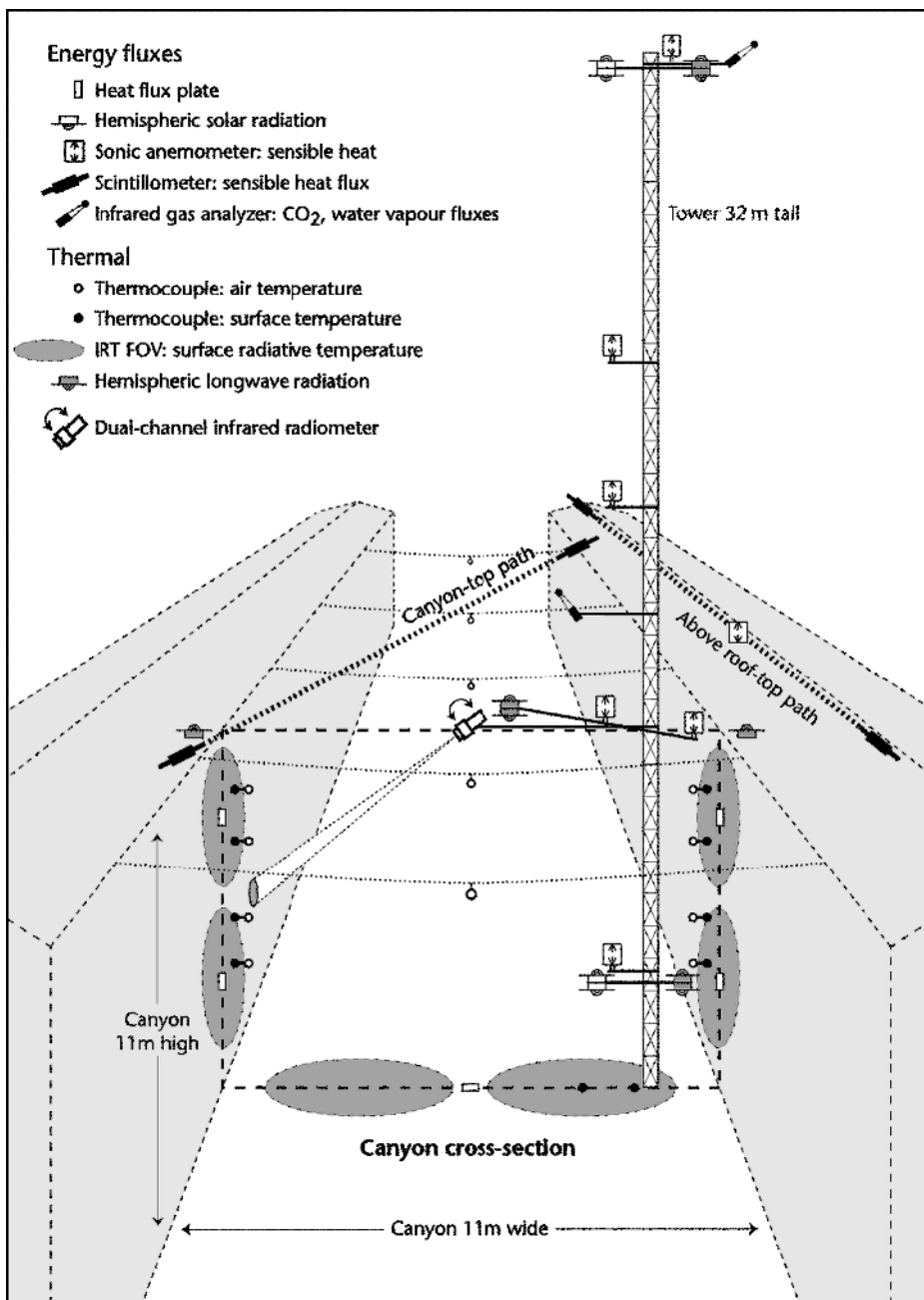


**Fig. 12.** Conceptual representation of the Sperrstrasse canyon (see also Fig. 11) showing instrumentation to monitor the thermal character and energy fluxes at the cross-section near the tower. The temperature sensors monitored the thermal status of its walls and in the air down the canyon axis, and the flux sensors measured the fluxes of momentum, heat and moisture into and out of the canyon volume

**Table 4.** Additional observations concerning street canyon energetics at site Ue1 during the IOP

Objective	Specific goal	Instruments/means	Comments	Reference
Surface thermal characteristics of canyon facets	Surface and air temperature profiles.	Type-E 36 awg thermocouples on walls; also canyon floor, asphalt road and sidewalk	Air temp.: 0.1 m distance from wall, shielded for radiation	Voogt and Oke (1991); Fairey and Kalaghchy (1982)
	Radiative surface temperatures	15° FOV non-scanning infrared thermometers (IRT; Everest Model 4000.4GL)	Canyon walls and roofs monitored	
Radiation	Long-wave radiation through the canyon top	Eppley pyrgeometer (Model PIR)	Mid-canyon position, boom from tower	
	Downward long-wave radiation	Pygeometer	North and south sides of the canyon, also: top of tower	
	Canyon surface radiative temperature	1 FLIR SC 500 (portable thermal scanner)	Various positions, often along-canyon	e.g., Fig. 12
Air temperature	Radiative flux divergence <i>within</i> canyon	1 AGEMA Thermovision THV900 DCIR	South-facing wall monitored Mid-canyon position, top of canyon	See text
	Additional to tower	Along canyon line of sensors Short-term traverses down the canyon	Near roof level portable mast	
In-building air temperature		thermistor/mini data logger packages	Each side of canyon, in stairwells	

previously available, including the ability to make some assessment of canyon surface emissivities.

A unique feature was the deployment of a dual-channel long-wave radiometer (DCIR) mounted above the center of the canyon, approximately at the height of the top of the walls, to measure nocturnal radiative flux divergence in the canyon air. DCIR is a prototype radiometer developed by Dr. Manuel Nunez of the University of Tasmania. When aimed at a target (here a wall or the floor of the canyon) it measures the radiative temperature in its Field of View (FOV) in two separate channels of the electromagnetic spectrum due to the introduction of a filter. Differences between the signal with, and without, the filter allow calculations of long-wave radia-

tive flux divergence of the canyon air in the path. The orientation of the DCIR was rotated through a number of angular steps to allow a scan of the entire canyon cross-section (one complete scan took 20 min). This part of the study seeks to better understand the fundamental processes underlying the urban heat island effect. To do so we are using modern precision radiometry technology that was not available at the time of the only other such study by Nunez and Oke (1976).

#### 2.4.3 Flux exchanges between the UCL and the overlying air

The SC site provides the opportunity to study the exchange of heat, mass and momentum between

the canyon volume and the above-canyon flow in more detail than has been previously possible. For the duration of IOP two CO<sub>2</sub>/water vapor flux sensors (Licor, model 7500) were added to the available instrumentation; one at the top of the mast (at 31.7 m) and another over the street near the top of the canyon (at 14.7 m) (Fig. 12). With this arrangement it is possible to study the vertical variation of the turbulence statistics and fluxes throughout and just above the RS and their representation within a *local scaling framework*. Hence local similarity functions can be derived for the urban RS, and energy transport through coherent structures can be investigated. Very few urban studies have included the measurement of CO<sub>2</sub>, although cities are known to be a major source of this greenhouse gas, which has implications for local air pollution and global climate issues. The present flux observations allow analysis of the temporal dynamics of urban CO<sub>2</sub> exchanges (Vogt et al., 2003; Roth et al., 2003) and CO<sub>2</sub> will be also used as a tracer to examine the patterns of heat transfer for carefully selected cases.

Horizontally representative turbulent fluxes are extremely difficult to obtain in the RS where the mosaic of rooftop and street canyon surfaces present a particularly complex three-dimensional surface. Little is known about the actual spatial heterogeneity of turbulent fluxes within the RS, nor the relative importance of rooftop versus street canyon characteristics in determining the turbulent structure of the UBL. To address such questions two small aperture scintillometers (Scintec, Model SLS 20) were installed near the SC tower during the IOP (Fig. 12). One was installed around roof-level at 15.8 m above street level (with an optical path of 116 m, diagonally across the street canyon). The second path of 171 m was located at 19.3 m agl, which was approximately 3–5 m above the varied roof height along the path.

Scintillometers have been shown to be effective tools for the measurement of spatially averaged turbulent fluxes over both homogeneous (De Bruin et al., 1995) and heterogeneous surfaces (Kanda et al., 2002; Lagouarde et al., 2002; Weiss et al., 2002). Further, as a result of the spatial averaging of the turbulent eddies it is possible to use shorter averaging times in the calculation of fluxes (De Bruin et al., 2002), which is particularly advantageous in heterog-

eneous environments where constraints of stationarity may not be met for prolonged periods.

The validity of the assumptions underlying calculation of sensible heat fluxes using the parameters measured by a scintillometer, may be problematic in the urban atmosphere. Line-averaged turbulent fluxes are calculated from the refractive index structure parameter ( $C_n^2$ ) and the inner scale ( $l_o$ ) using Monin-Obukhov similarity theory (MOST). However, MOST cannot be applied directly in the urban RS (Roth, 2000) and a modified form of these equations such as that developed by Kanda et al. (2002) for Tokyo may be utilized. BUBBLE data will be used to further analyze and validate the possible universality of these equations. They rely – among others – on accurate measurements of height above the surface. For the near rooftop interface estimation of this height becomes problematic (Salmond et al., 2003) and will have to be addressed.

The observed parameters  $C_n^2$  and  $l_o$  depend on a weighting parameter with largest weight near the mid-point of the pathway. Hence, a 3-D sonic anemometer was placed at the mid-point of each path. Figure 13a shows good correlation between the turbulent heat flux  $Q_H$  from the canyon sonic at 14.7 m and the canyon scintillometer. The increased spatial averaging of the turbulent eddies in the scintillometer fluxes gives a smoother diurnal cycle than the point measurement. Interestingly, the nighttime heat fluxes (which are always positive) from the scintillometer are consistently higher than the sonic values. This may reflect the improved spatial averaging of the scintillometer data. On the other hand the daytime scintillometer values tend to be equal to or smaller than the sonic values. Figure 13b illustrates that  $Q_H$  from the rooftop scintillometer tends to be slightly larger during day- and nighttime than the rooftop sonic. Note that possibly such detailed comparisons are not warranted until issues associated with the effective height of measurement are refined. However, detailed analysis of the results (Salmond et al., 2003) shows that scintillometers are useful tools for the measurement of turbulent heat fluxes in the RS. In the complex zone near the rooftop interface, path-averaged data from scintillometers may provide more spatially representative measurements of turbulent heat fluxes from

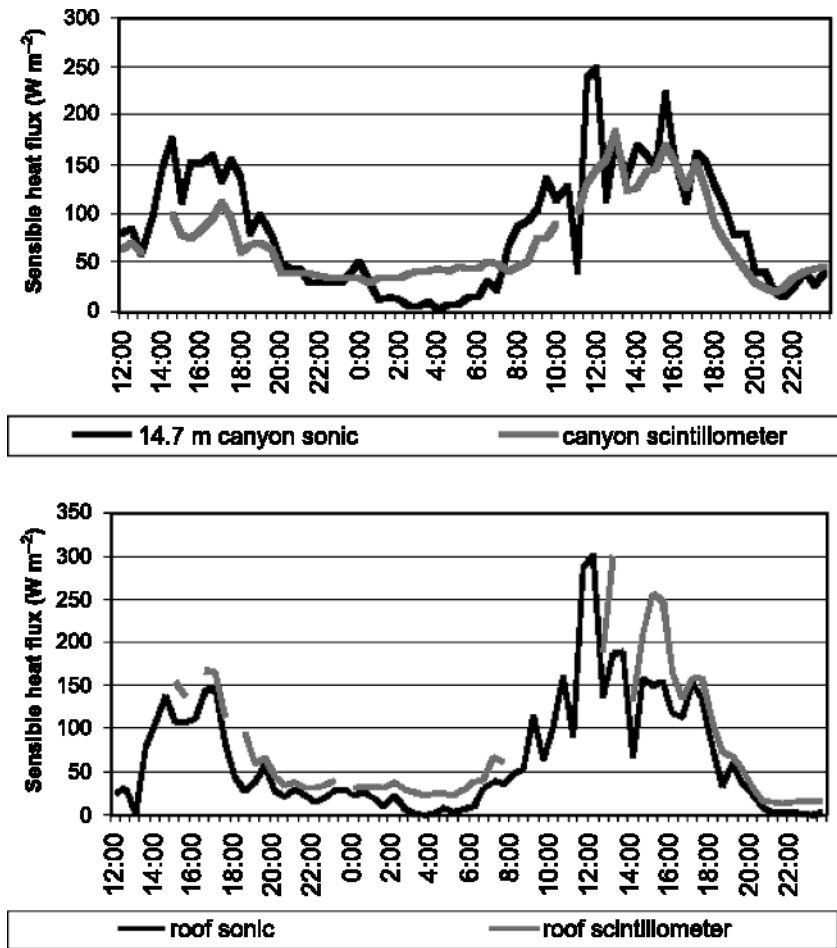


Fig. 13. a) Comparison of the sensible heat fluxes ( $Q_H$ ) from the canyon scintillometer and 14.7 m canyon sonic anemometer, between 12:00 July 6–23:00, July 8 2002, and b) from the roof top scintillometer and roof top sonic anemometer for the same period (all times in CET)

different urban surfaces compared to traditional single point eddy covariance approaches.

#### 2.4.4 Satellite ground truth

Research on the urban heat island with different thermal satellite data for various cities has been conducted by Munier and Burger (2001) for Berlin, Nichol (1998) for Singapore, Parlow (1998, 1999, 2003) for Basel, Anielo et al. (1995) for Dallas, TX; Gallo et al. (1993), Dousset and Kermadi (2003), Dousset and Gourmelon (2003) for Marseille and Paris and many others. With in-situ measurements the radiation balance can only be measured for point locations and not over the whole urban area. But heat fluxes can exhibit a large heterogeneity over urban areas. One option is therefore the application of satellite remote sensing of the solar and terrestrial wavelengths in combination with modeled atmospheric corrections. A first goal of BUBBLE-SARAH (Satellite Analysis of Radiation And Heat Fluxes)

is to compute the spatially distributed net radiation as a key factor for heat flux studies. Short-wave reflection and long-wave emission can be computed from multi-spectral satellite data. Solar irradiance and atmospheric counter radiation are integrated from numerical model results.

Satellites with different spatial, temporal and spectral resolutions are being used in this project. The present research will focus on Landsat 7 ETM+, which has the unmatched resolution of 60 m in the thermal IR-band, offers the possibility to compute albedo with a resolution of 30 m and possesses a panchromatic band with 15 m resolution. In addition, use will be made of TERRA-ASTER data with a spatial resolution of 15 m in multi-spectral visible channels. The infrared band has a stereo viewing capability and digital elevation can be computed from these data. The MODIS and NOAA-AVHRR offer a fairly good temporal resolution of several orbits per day but have a poor spatial resolution of 1000 m.

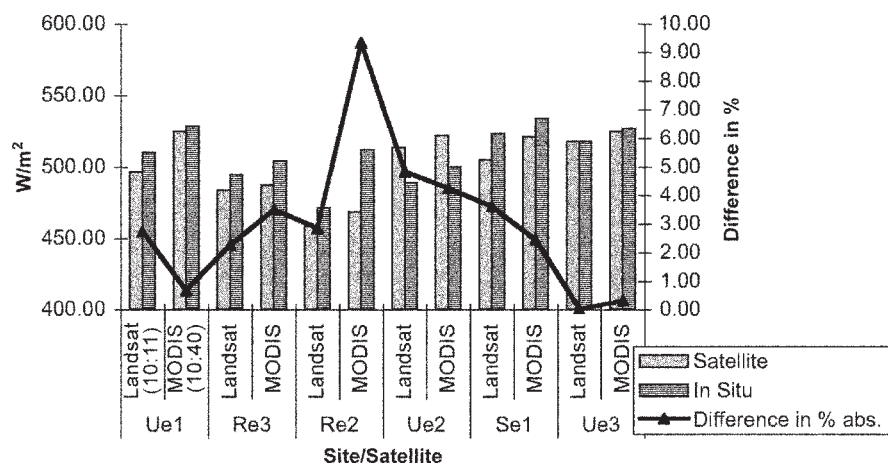


**Fig. 14.** Comparison of satellite derived and in-situ long-wave emissions (station labels as in Table 1), columns and left scale. Difference in percent: solid line, right scale. The site symbols (Ue1, Re1, etc) correspond to those in Fig. 2

With the available radiation measurements from the many BUBBLE sites, it is possible to compare and calibrate the satellite data with ground measurements. Long-wave emission ( $L \uparrow$ ) and modeled short-wave reflection can be validated with in-situ measurements. An example is given from the Landsat 7 image of 8 July 2002. The thermal band 6 (low gain) has been transformed into  $\text{Wm}^{-2}$  and an atmospheric correction after Price (1983) has been applied. For the atmospheric correction a high-resolution (25 m raster) a digital elevation model of SwissTopo has been used in combination with a radio sounding from Payerne, some 50 km to the southwest of Basel. In addition, MODIS data of the same day (11:40 CET) are also used. A comparison with in-situ measurements is presented for sites Ue1, Ue2 and Ue3 (urban), Se1 (suburban) and Re2, Re3 (rural) in Fig. 14. These sites represent important land use classes of the Basel region. For MODIS sites Re1 and Re4 (rural) are used too.

Differences between in-situ measurements and the satellite-retrieved data are very small, ranging from 0 to 9.5% (Fig. 14). Note that the in-situ instruments have an uncertainty of at least  $5\text{--}10 \text{ Wm}^{-2}$  ( $\approx 1\text{--}3\%$ ), even with very good calibration. Hence, the satellite measurements are in excellent agreement, especially for MODIS with its sensor resolution of only 1000 m. The accuracy of Landsat is slightly better than that of MODIS (2.9 to 3.1%). The two sites Re2 and Ue2 show the largest differences, almost double those at the other sites. The reason for this behavior has yet to be determined.

Some preliminary analysis has been carried out after correction and calibration of the acquired data. High-resolution satellite data and numerical models are used to study the spatial distribution of radiation fluxes and the net radiation (Parlow, 1999 for detailed information). Figure 15 shows  $L \uparrow$  (upper panel) and the computed net radiation  $Q^*$  (lower panel) for the city of Basel on July 8, 2002 at 11:11 CET as one first result of this project. The airport, the industrial sites and the city center can easily be identified by large  $L \uparrow$  up to  $530 \text{ Wm}^{-2}$ . The terrestrial emission of the sealed surfaces of the city varies within a range of  $\pm 40 \text{ Wm}^{-2}$ . Due to this high radiative energy loss these surfaces have a lower net radiation.  $Q^*$  at the airport in the north-western part of the image is partly below  $300 \text{ Wm}^{-2}$  due to high surface temperatures and high albedo values there. Both data sets are highly correlated ( $Q^* = -1.36L \uparrow + 1185.7$ ) with a correlation coefficient  $R = -0.825$ .

The main focus for further research will be on the analysis of radiation fluxes, net radiation and heat fluxes as a function of urban surface parameters like sky view factor, street canon width-to-height ratio etc. and on the diurnal variation of energy and heat fluxes based on MODIS and NOAA-AVHRR data.

### 3. The BUBBLE tracer experiment

#### 3.1 Overview

Within the framework of BUBBLE and taking advantage of the wealth of meteorological information available, a series atmospheric dispersion

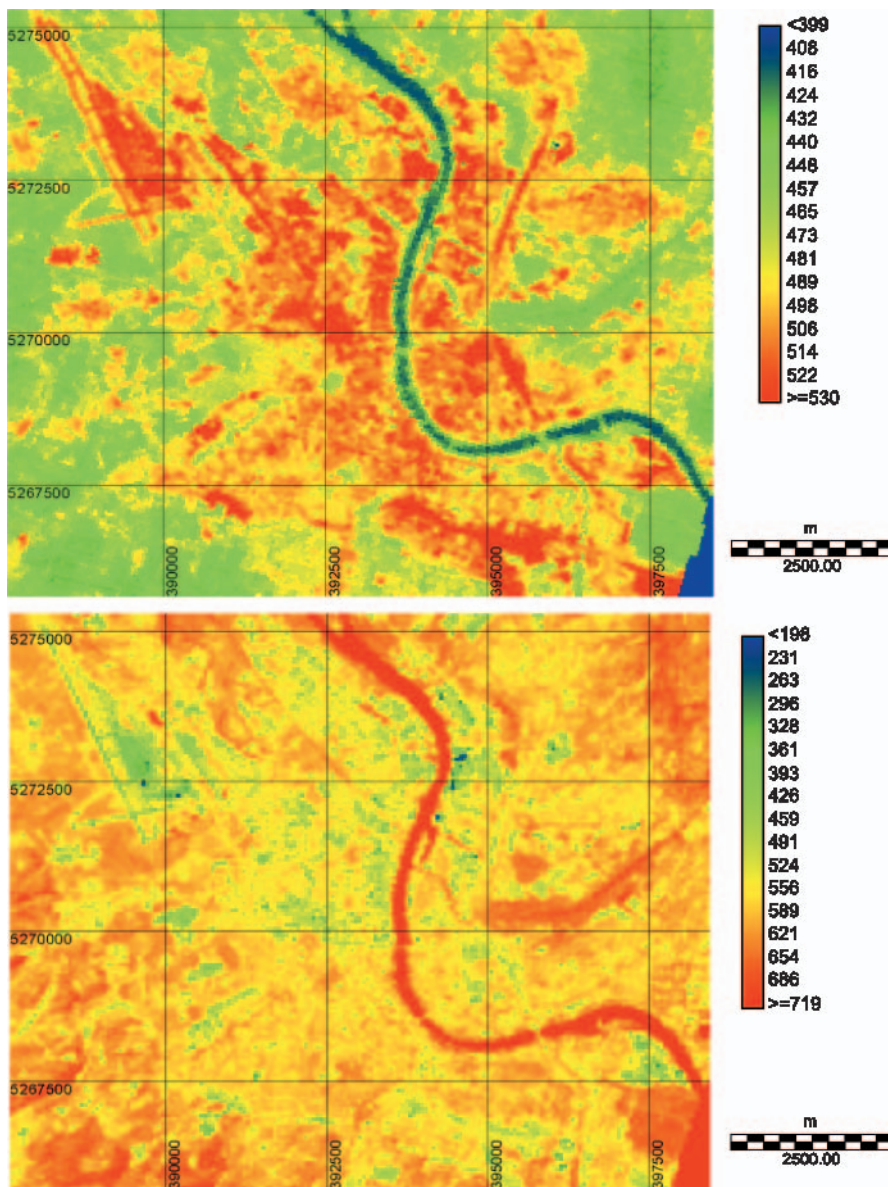


**Fig. 15.** Long-wave emission (upper panel) and net radiation (lower panel) for July 8, 2002 at 11:11 CET of the city of Basel

experiments were carried out. Both, the tracer release and sampling sites were located near roof level, above and outside the street canyons. As a tracer gas Sulphurhexafluoride ( $\text{SF}_6$ ) was used. Due to logistic difficulties in a city, tracer samplers cannot be laid out in predefined arrays downwind of the source location according to the prevalent wind direction. Rather, arrangements have to be made beforehand and flow conditions according to the layout have to be awaited. Due to topographical features of the city a thermal wind system develops on cloud free summer days that creates a northwesterly flow in the afternoon – called Clara Wind. The design

of the experiment was done according to this thermal wind system.

The experiments were carried out in a fairly homogeneous part of the city near sites Ue1, Ue3 and Ue4. The tracer  $\text{SF}_6$  was released from the roof of a parking house at about 1.25 times the average local building height. In one occasion the tracer release had to be made from a mobile crane at a different position. Samplers were located in a downwind sector of about  $90^\circ$  opening angle and located at 1.5 m above roof level, typically 15 m above the street. For most of the tracer releases samplers were located on two approximate arcs at 700 and 1000 m distance

from the source. Additionally, a profile along the centerline of the expected plume extended up to about 2.4 km (Fig. 17). The release of tracer started 60 min prior to the sampling and was kept constant. Sampling was performed in bags, of which 6 were filled in sequence at each location with a filling duration of 30 min for each. Thus a time series of 6 half-hour averaged values of near-roof concentrations is available at each of the sampling sites. Bags were subsequently analyzed in the laboratory and a background concentration that was measured for each release separately in the experimental area was finally subtracted from the analyzed concentrations. Reproducibility of the observed concentrations was excellent. More detail about this tracer experiment can be found in Gryning et al. (2003, 2004) and Rotach et al. (2004).

### 3.2 Overview of the releases

A total of 4 tracer experiments were carried out, all characterized by low wind speeds and predominantly convective conditions. It is an interesting feature of the present experiments, that in three of the cases the convective velocity  $w_*$  is larger than the mean wind speed, and always larger than the mechanical scaling velocity (Table 5). The low wind speed distinguishes these experiments from most other tracer experiments (Batchvarova, 2003). The prediction of the mean wind direction was a real challenge from a logistic point of view as only minor perturbations in the large-scale pressure field could shift the ther-

mal Clara Wind tens of degrees away from its prevailing direction. Additionally, the wind was very variable both in time and space during the tracer releases. In this respect the 6 half-hourly time series of tracer samples yields information on the variability of the concentration field within a Clara Wind event.

Table 5 gives an overview on the meteorological conditions during the four experiments. With the exception of the experiment on July 4 all took place under (strongly) convective conditions. Nevertheless, all the experiments are characterized through a substantial *mechanical scaling velocity*,  $\hat{u}_*$ , due to enhanced mechanical turbulence over the urban surface. Here,  $\hat{u}_*$  was determined from the *profile* of Reynolds stress at site Ue1, by a fitting procedure according to Kastner-Klein and Rotach (2004), which determines the *maximum (norm) Reynolds stress*. It is assumed that this maximum Reynolds stress corresponds to the effective stress the flow sees over an urban surface (see Rotach, 2001).

### 3.3 Preliminary results

The large spatial and temporal variability of the wind field in the experimental area and the effect it has on the dispersion of the tracer plume is illustrated for the 26 June experiment in Fig. 16. In the upper panel a proper Clara Wind situation (wind direction about  $330^\circ$  over the tracer release area) is shown with a strong plume centerline and large near-source concentrations. 90 min later the (very weak) wind at the release point has changed

**Table 5.** Meteorological conditions during the 4 tracer experiments; averaging times are shown in CET. Here, the height  $z_m$  denotes the height of maximum fitted Reynolds stress according to Kastner-Klein and Rotach (2004). From the Reynolds stress profile at this datum  $\hat{u}_*$  is determined to serve as a characteristic velocity and  $z_m$  is interpreted as the height of the roughness sublayer (Rotach, 2001),  $\bar{u}$  stands for the mean wind speed,  $w_*$  is the convective velocity scale that has been determined using the turbulent heat flux from an average of the two top-most levels at site Ue1. Finally,  $z_i$  is the height of the UBL

Experiment	$z_m$ [m]	$\bar{u}$ [ms <sup>-1</sup> ]	$\hat{u}_*$ [ms <sup>-1</sup> ]	$w_*$ [ms <sup>-1</sup> ]	$z_i$ [m]	Conditions
26 June 13:00–16:00	21.7	1.28	0.41	2.31	1809	Strong convection, steady wind direction
4 July 15:00–18:00	24.0	2.49	0.60	1.77	1286	Westerly, fairly strong wind, cloudy
7 July 14:00–17:00	19.2	1.44	0.31	2.22	1867	Partly cloudy, strong convection
8 July 15:00–18:00	20.4	1.78	0.41	2.27	1312	Clear sky, convective

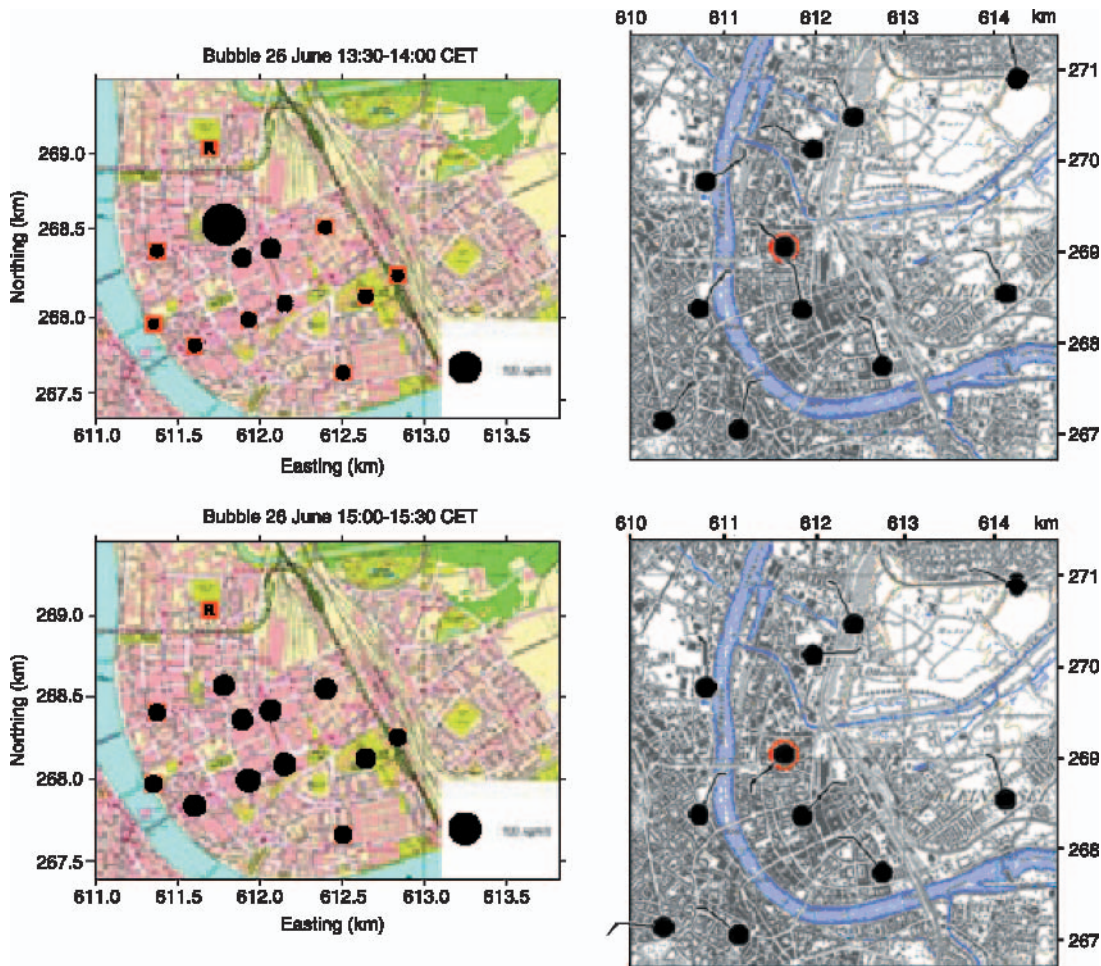


**Fig. 16.** Illustration of two sample half-hourly averaged tracer concentrations and the wind field for the experiment on 26 June 2002. In the left panels the release point is marked with R; at the tracer sampling positions the measured concentration is indicated with the area of the filled circle. For comparison, a filled circle representing  $100 \text{ ngm}^{-3}$  is shown in the white box. In the right panels the release point is drawn with a red circle. The wind barbs indicate wind speed and direction with the following convention (example: wind from SW): ● Wind speed  $< 1 \text{ ms}^{-1}$ ; ⚓ Short barb:  $1 \text{ ms}^{-1}$ ; ⚓ Long barb:  $2 \text{ ms}^{-1}$ . Base map (c) copyright GVA BS, 25102002

direction by almost  $90^\circ$  and the tracer distribution for that period was much more uniform. Figure 17 shows the tracer concentration field averaged over the 3-hour sampling time and a consistent structure in the plume appears (Gryning et al., 2003). This illustrates that the considerable variability in the wind on the time scale of half an hour is markedly reduced on a 3-hourly basis.

Some of the salient features of the BUBBLE tracer experiments are outlined in Rotach et al. (2004) and will only briefly be summarized here:

- Despite the irregular nature of the urban surface and the low release height a clearly plume-like near-surface concentration pattern emerged from the observations (see also Fig. 17).

- Interpolated concentrations yield a near-Gaussian distribution in the horizontal plane (Gryning et al., 2003). On average, and for all the tracer experiments, the plume width  $\sigma_y$  is *underestimated* using  $\sigma_y = \sigma_v t f_y(t/T_Y)$  and  $T_Y = 200 \text{ s}$  (recommended for surface sources) or  $T_Y = 600 \text{ s}$  (recommended for elevated sources). Here,  $f_y$  is a semi-empirical function,  $t$  is the travel time,  $T_Y$  the Lagrangian integral time scale,  $\sigma_v^2$  the lateral velocity variance. However, if  $T_Y$  is estimated from  $T_Y = z_i/\sigma_v$ , where  $z_i$  is the Mixed Layer height, quite good agreement between observation and estimation is obtained. Clearly, the present data set will allow for directly deter-

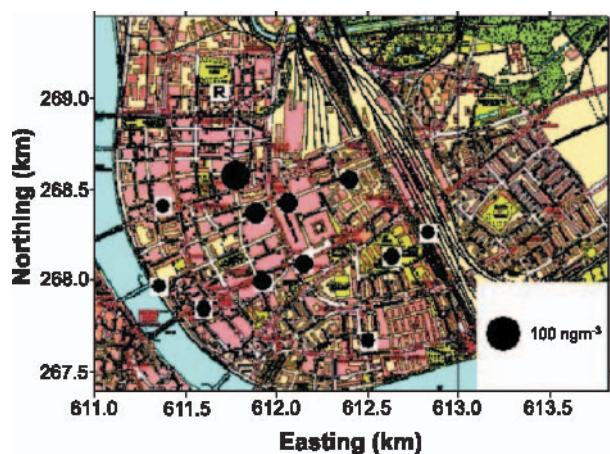


**Fig. 17.** Tracer concentrations on 26 June 2002, 1300–1600 CET. Further explanations as in Fig. 16. Base map (c) copyright GVA BS, 25102002

mining  $T_Y$  from the spectra, so that this issue can be investigated in more detail.

- About 700 m downwind of the source location, at site Ue1 three levels of concentration measurements were taken at 3, 10 and 17 m above street level (local roof level was 15.1 m). Figure 18 shows that on average and also for individual profiles, only small vertical gradients are present. This indicates that a considerable part of the tracer enters the canyons (without destroying the Gaussian-type lateral dispersion); also the contribution of non-local sources in a street canyon leads to largely well-mixed concentration patterns.

The BUBBLE tracer experiments are discussed in the wider context of other recent urban disper-

sion studies in Batchvarova and Gryning (2004, 2005) and Gryning and Batchvarova (2004).

## 4. Numerical modeling

### 4.1 Urban surface exchange parameterization

In this study a meso-scale wind model adapted for urban areas (Finite Volume Model, FVM, Clappier et al., 1996) is applied. The FVM model was used to develop and test a new urban turbulence parameterization (Martilli et al., 2002, 2003). In this parameterization the model domain starts at the street level (where large parts of pollutants are emitted). The city is represented as a series of buildings of the same size with equal distance but with different heights (i.e. the building density is a function of height). Depending on the building height and the vertical model resolution (usually 2 to 5 m), several grid levels are defined below the average roof height. Extra terms representing the impact of the urban surfaces (roof, walls and street) are introduced in the momentum, energy and TKE equations of the model. For example in the momentum equation a term representing drag due to the walls is introduced as well as friction on the roofs and at street level (see Martilli et al., 2002 for details). For every grid cell, it is possible to define several street directions, and the results are then averaged over all the street directions. The model is also able to calculate the temporal and spatial concentration evolution of a tracer, and thus to support a tracer field experiment.

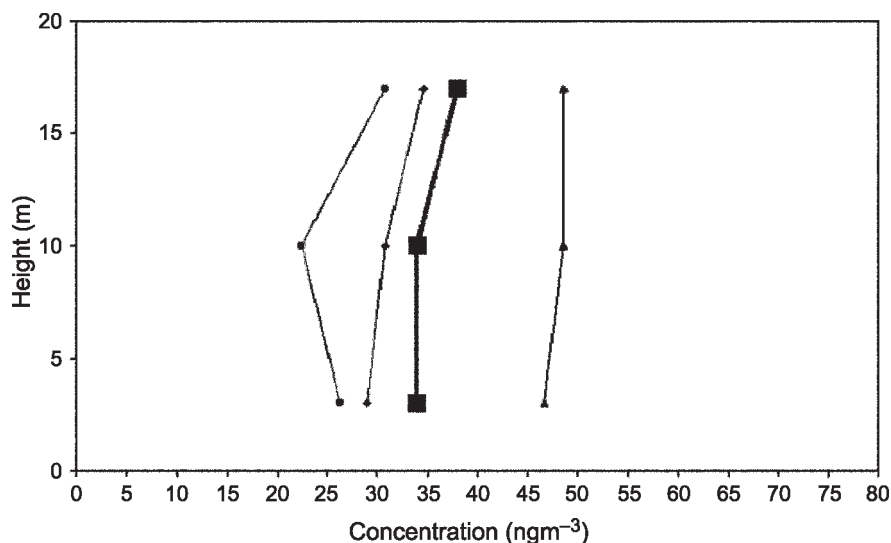


**Fig. 18.** Profiles of tracer concentration at site Ue1 about 700 m downwind of the source location (site Ue4 in Fig. 2). Data from experiment #1 (26 June 2002), 13–14 CET (●), 14–15 CET (▲), 15–16 CET (◆) and averages over the whole period (bold line and symbols). The height of mean roof level in the tracer area is 15.1 m

This new urban parameterization was tested using the BUBBLE measurements from site Ue1 (Roulet et al., 2003, 2004; Roulet, 2004). The simulations are performed first with a single column approach, in order to test the urban module offline. The boundary conditions at the top of the street canyon are taken from measurements at the top of the tower ( $\sim 30$  m above the ground). The model calculates fluxes and meteorological variables from this point down to the ground. The calculation and validation is applied to the urban RS, which is the crucial place for the influence of an urbanized scheme on the PBL structure. Input parameters for the city and building shape are chosen according to Table 1.

In order to test the urban module, and to quantify its impact on the meteorological modelling, three different simulations are carried out. The first (*urban*) uses the urban surface exchange parameterization as described above (percentage of rural areas set to zero). The second (*rural*) simulation considers a 100% rural soil coverage, while the third simulation (*traditional*) represents the traditional less detailed approach to represent urban surfaces used in meso-scale models (modification of only the roughness length and the soil thermal capacity). The example presented here is for 25 June to 16 July 2002, and corresponds to the second half of the IOP.

Average profiles of potential temperature in the street canyon are fairly well represented by the urban module (Fig. 19). At night-time, *rural* and *traditional* simulations are not able to capture the heat storage near the ground, whereas the *urban* simulation indicates a temperature at the ground very close to the measurements (and 4–5 K higher than *rural* and *traditional* at midnight). It is thus able to represent the nocturnal heat island over the urban area. During daytime, the shape of the profile from the *urban* simulation is in better agreement with the measured profile, but with an offset of 1–2 K (profile at 12:00 and 18:00 LT). The profiles of the kinematic heat flux  $\overline{w'\theta'}$  (Fig. 20) from the *urban* simulation are different than those from the traditional method. While  $\overline{w'\theta'}$  is more or less constant over the entire UCL in the *traditional* simulation (as prescribed by the surface layer theory, which doesn't hold in the RS), it increases with height in the urban simulation. This trend is observable for both night and daytime.

The vertical heat flux is slightly negative during night-time in the traditional simulation, while it is near zero or slightly positive in the urban simulation and in the measurements. This means that the cooling is smaller with the urban parameterization than with the traditional method, which is in agreement with the higher temperatures computed during night-time with the urban module (Fig. 19). Additional work (not reported here) analyzes the impact of each input term of the module, in order to determine the most sensitive parameters (Roulet et al., 2004), and eventually to improve the quality of the simulation. Also three-dimensional simulations on the region of Basel, in order to validate the meso-scale model with the urban parameterization are performed (Roulet, 2004).

#### 4.2 Dispersion modeling

If pollutant dispersion modeling cannot afford full 3d-simulations (for example because many situations need to be simulated or the result needs to be available in short, emergency responding time) simpler dispersion models may be used. In recent years a number of models have been developed which are specifically suited for urban surfaces. Rotach (2001) has modified a Lagrangian Particle Dispersion Model (LPDM) to specifically take into account the *turbulence structure of the urban RS*. An even simpler dispersion model to be tested on the BUBBLE tracer data is the Gaussian plume model OML-URB. This model is based on the Danish operational dispersion model OML (Olesen et al., 1992) and has been modified for urban RS turbulence in very much the same fashion as the LPDM by De Haan et al. (2001). Using yearly average concentration data from many sites in Zurich (Switzerland), they also found that taking into account the turbulence structure of the urban RS largely improves the prediction skill of this simple dispersion model. The same conclusion is drawn by Leone et al. (2002) using a Gaussian model to model tracer releases (surface source) in the context of URBAN2000 in Salt Lake City.

Figure 21 shows that numerical modeling using an urban LPDM is able to reproducing near-surface observations satisfactorily, at least for experiments 1 and 2. Clearly, these two

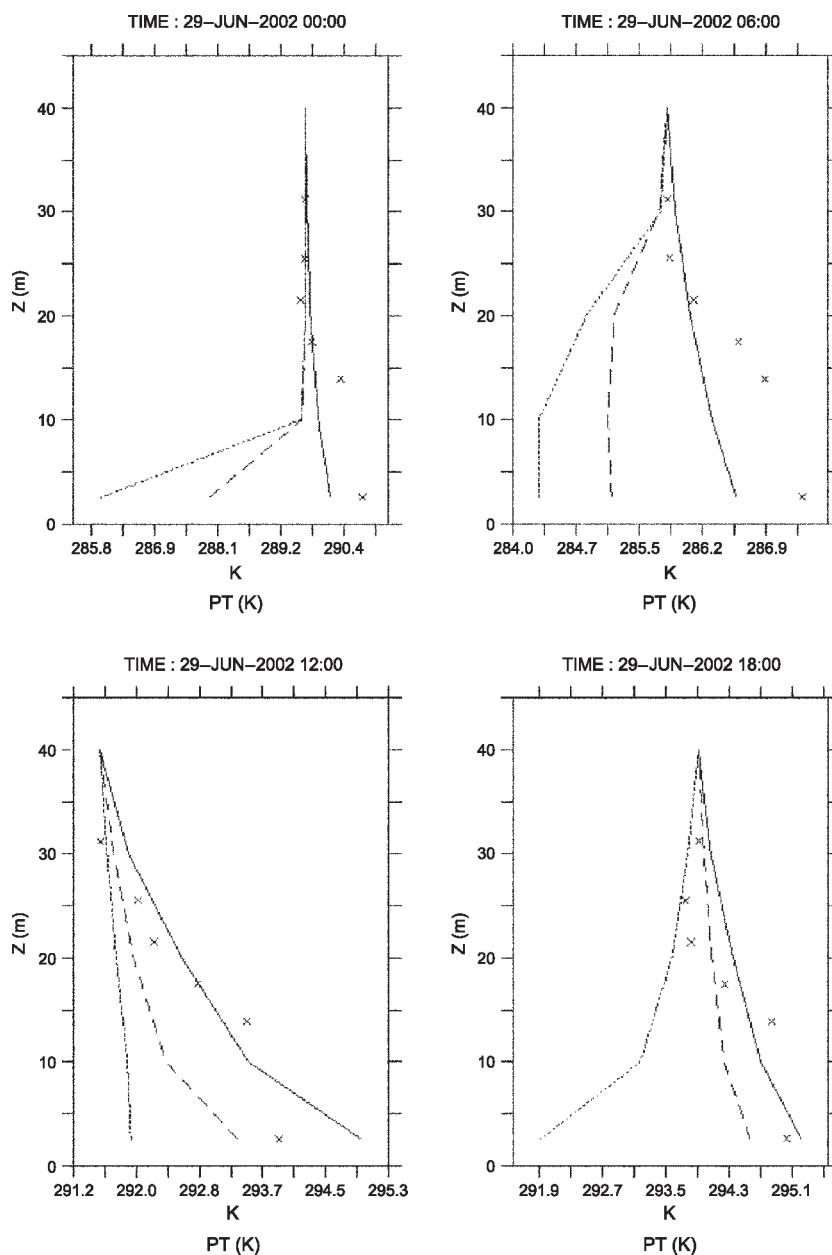


**Fig. 19.** Daily evolution of potential temperature (denoted PT) in the street canyon for the urban simulation (solid line), the rural simulation (dashed line), the traditional urban parameterization (dotted line) and the measurements (crosses) in the street canyon. Observations from site Ue1

experiments are reproduced better than 3 (large scatter) and 4 (underestimation by the model). Overall the model has a tendency to underestimate peak concentrations and overestimate small concentrations (i.e. at large distances from the source). This points to a (modeled) *under-estimation* of the lateral dispersion process – even if observed turbulence characteristics (such as  $\sigma_v$ ) are employed and the model takes into account the specific characteristics of urban RS turbulence (Rotach, 2001). Possible reasons for this underestimation and more detail about the simulations are given in Rotach et al. (2004). Here, it

suffices to state that the BUBBLE data set is excellent to study a) urban dispersion processes in general and b) to validate and improve dispersion models for urban applications.

## 5. Wind tunnel simulations

### 5.1 Introduction

There is a growing awareness within the scientific community that validation data for numerical models are not *just any* experimental data. They must fulfill certain requirements with respect to

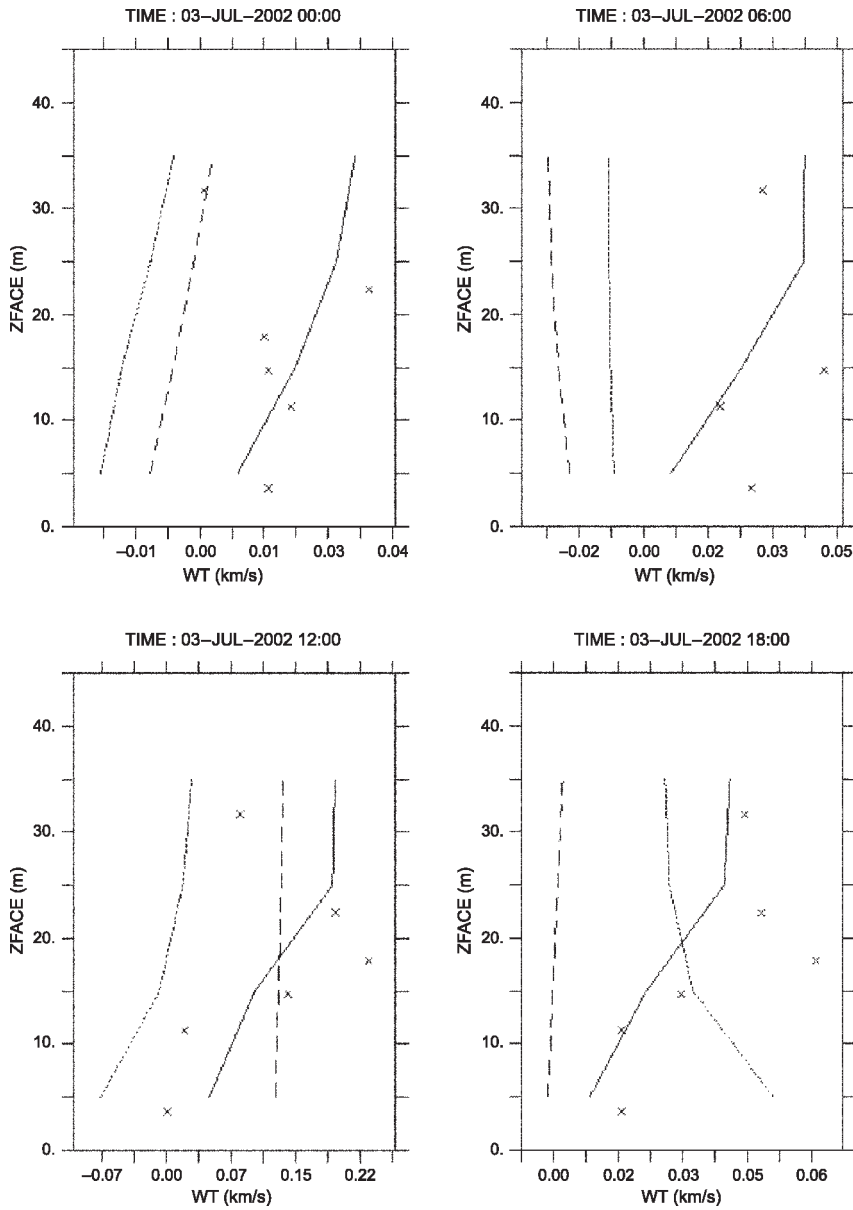


**Fig. 20.** Daily evolution of the kinematic vertical temperature flux (denoted WT) in the street canyon for the urban simulation (solid line), the rural simulation (dashed line), the traditional urban parameterization (dotted line) and the measurements (crosses). Observations from site Ue1

completeness, spatial and temporal resolution, accuracy and representativeness of the measured results (Leitl, 2000). If these requirements are not met, too many degrees of freedom remain for the set-up of numerical model runs. A wide variety of numerical results can be generated within the limits of reasonable assumptions for the input data, with the consequence that a tenable conclusion concerning the model quality cannot be achieved.

To overcome these problems, the best solution is the *combination of field measurements and laboratory experiments*. Modern boundary layer wind tunnels allow the replication of certain urban flow and transport processes under

carefully controlled conditions (Schatzmann et al., 1999 or Pascheke et al., 2001). On the one hand, physical modeling allows for reducing the gaps in inevitably fragmentary field data and the requirements stated before can be met thus significantly enhancing the value of the field data. On the other hand, physical models are always limited due to scaling considerations (trade-off between detail and similarity requirements) and stratified flows are still at least difficult to simulate. Therefore, the full-scale BUBBLE observations were complemented by a wind tunnel study of a core region in the city of Basel. Wind tunnel runs include both flow (turbulence) characteristics and concentration

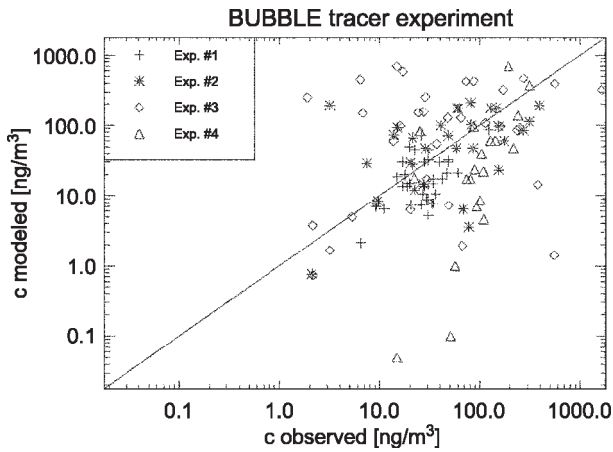


**Fig. 21.** Comparison of modeled and observed 1-hr mean near-roof concentrations for all four tracer experiments (see inlet). Difference to the results presented by Rotach et al. (2004) for Exp 1 (their Fig. 11) is different choice for the parameter  $C_o = 2$  (rather than 3). See their discussion on the impact and meaning of this modification

measurements. The area of interest has therefore been defined as the region of the full-scale tracer experiments (Section 3) and any mentioning of specific conditions will refer to the tracer experiments (Section 3).

### 5.2 The Hamburg wind tunnel

The physical model study for BUBBLE is carried out in the new Large Boundary Layer Wind Tunnel WOTAN at Hamburg University (Fig. 22). The 25 m long facility provides an 18 m long test section equipped with two turntables and an adjustable ceiling. The cross section of the tunnel measures 4 m in width and 2.75 to 3.25 m in height (variable ceiling). For precise probe positioning and automated measurements, the tunnel has a computer controlled probe carriage system featuring a positioning accuracy of about 0.1 mm on all 3 axes for all types of probes used in the tunnel. An extensive custom-made software package has been developed for automated and semi-automated measurements, probe calibration and positioning, online data visualization, data reduction and data validation.

In order to achieve high accuracy of wind tunnel data, all measurement systems, as well as the precision mass flow controllers for the emission sources can be calibrated against independent certified reference standards available in the laboratory. They are checked and recalibrated in order to ensure reliable measurements: at least

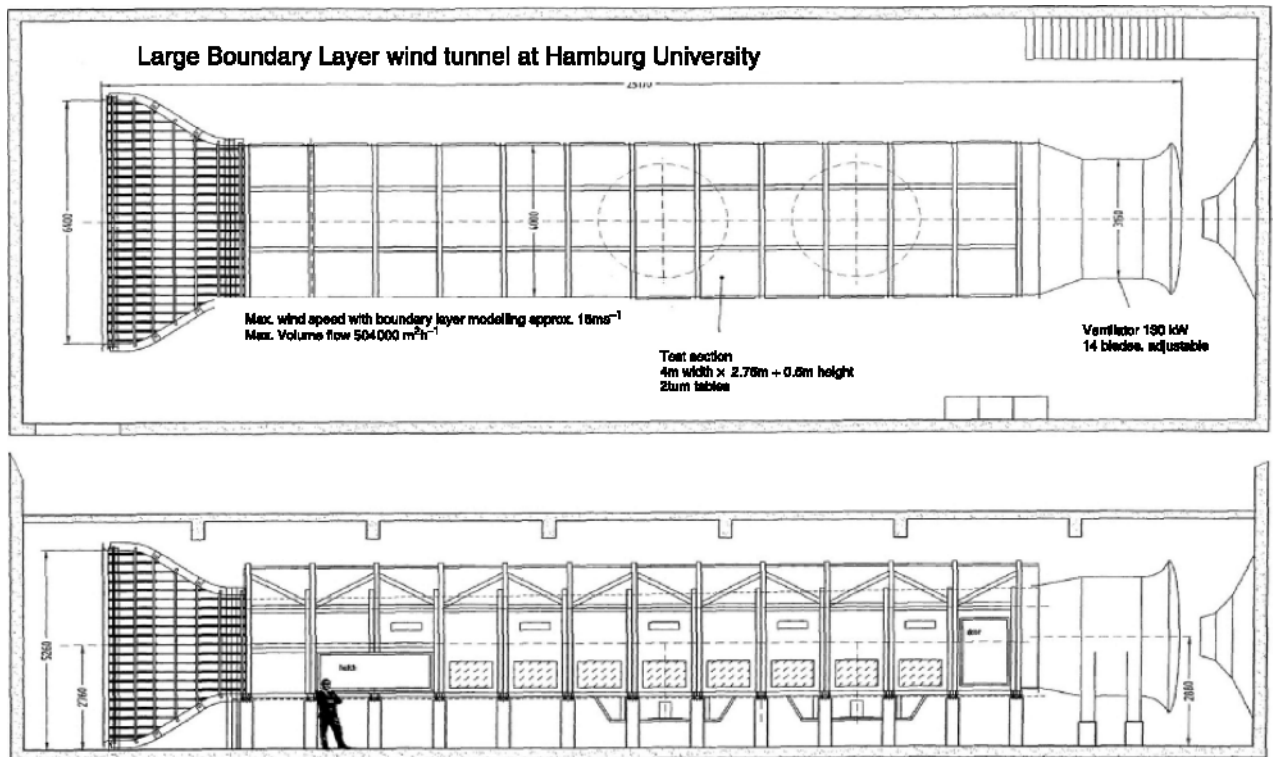


**Fig. 22.** Sketch of the Large Boundary Layer Wind Tunnel WOTAN of Hamburg University

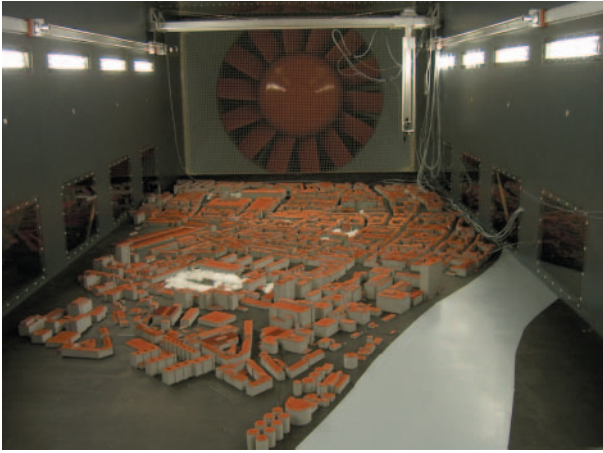


**Fig. 23.** Wind tunnel model (1:300) of the Kleinbasel area (corresponds approximately to the white area in Fig. 2). View from about  $330^\circ$ . The light surface region in the foreground represents the river Rhine. White material within the scale model corresponds to vegetation

once per day for the controllers and several times even between measurements for all other measurement systems.

### 5.3 Modeling considerations

A detailed aerodynamic model of the BUBBLE test site was constructed (Fig. 22). The geometric scale of the model was chosen to be 1:300. This scale allows an urban area with a diameter of about 1 km around site Ue1 to be represented in the wind tunnel. For the boundary layer flow to adjust to local conditions before entering the core area, the model will be extended a further 1 km into the prevailing wind direction ( $330^\circ$  – i.e. the dominating wind direction during the tracer experiments).

When choosing the geometric scale, one has always to compromise. The smaller the scale, the larger the area covered but the poorer the spatial resolution in a physical model. With the present choice, buildings of 30 m height have a model height of 0.1 m, which is well above tractable limits. Transferred to field scale, velocity measurements carried out with our Laser Doppler Anemometer are representative for a volume of about  $(0.15 \text{ m})^3$ , the spatial resolution of Fast

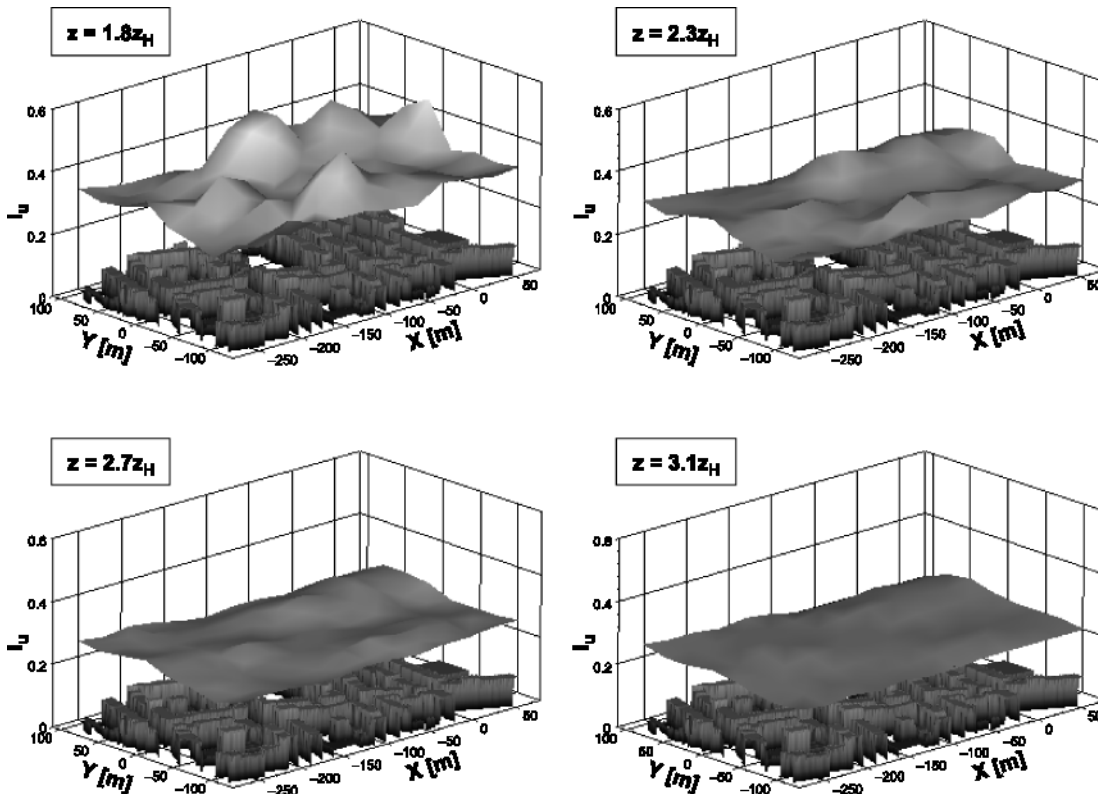


**Fig. 24.** Turbulence intensity at four height levels as observed over the wind tunnel model within the region where the tracer experiments took place. The approach flow is along the x-axis from left to right. Underlying building structures are indicated, site Ue1 is located at  $x = 0 \text{ m}$ ,  $y = 0 \text{ m}$

Flame Ionization concentration measurements is even better. Compared to the resolution of numerical grid models, the measurement volumes can be regarded as small.

For the simulation in the wind tunnel, field episodes with moderate to strong winds are chosen. Under such conditions it can be assumed that the vortices shed by the urban roughness elements are sufficiently intense to establish a well-mixed and neutrally stratified inertial sub-layer. Control over the boundary layer structure in the wind tunnel can be obtained by use of specific combinations of vortex generators and artificial roughness elements distributed over the bottom of the flow establishment section (upstream of the model domain).

#### 5.4 Preliminary results

The BUBBLE wind tunnel study aims at replicating and complementing the full-scale observations and at providing data suitable for the validation of obstacle resolving micro-scale models or for certain turbulent flux parameterization schemes used in such models. The total data set comprises a documentation of the boundary layer flow at the entrance of the model domain which consists of the mean flow profiles for all three components of the wind vector, the vertical and turbulent fluxes, the integral length scales of turbulence and the power spectral densities (Feddersen et al., 2003, 2004). As an example Fig. 24 shows the spatial distribution of the turbulence intensity  $I_u$  at four different height levels in the vicinity of site Ue1. Clearly on a quite small scale a substantial horizontal variability is observable close to roof level. At  $z/z_H = 3.1$  the turbulence intensity has homogenized significantly within the horizontal cross section. Also, flow visualization experiments were carried out using Laser light sheet technique and component resolving flow measurements at selected points of the model domain (field monitoring stations). Finally, in a second simulation phase high-resolution concentration measurements at selected points (again corresponding to full-scale tracer sampling sites) for several approach flow directions and for a variety of tracer gas release positions were obtained (Feddersen et al., 2004).

## 6. Summary and conclusions

In the present paper first results from the activities within the Basel UrBan Boundary Layer Experiment, BUBBLE are presented. The overall goal of this project was to address a number of unresolved issues in urban boundary layer meteorology as emerged from a series of workshops within COST 715 (Schatzmann et al., 2001; Piringer, 2001; Piringer and Kukkonen, 2002; Rotach et al., 2002, 2003a).

The philosophy of BUBBLE can be summarized as follows:

- To provide a long-term data set specifically suited to investigate the meteorological conditions determining pollutant dispersion processes in urban areas. Specifically, it was made sure not only to operate *either* near-surface turbulence observations *or* remote sensing boundary layer observations, *but both*. With this in mind two urban turbulence sites (6 levels each), a wind profiler and a lidar monitored the boundary layer in the City of Basel for a period of about one year.
- To investigate spatial inhomogeneity of features as emerging from the long-term observations through establishing many more sites during an IOP of about one month duration. This led to setting up additional surface (suburban and rural) turbulence as well as remote sensing sites (RASS, sodars, tethered balloon) in the area of Basel.
- To yield the background meteorological observations for a number of specific research topics in the urban environment. Thus during the IOP specific measurement campaigns were made with respect to urban street canyon energetics, exchange of CO<sub>2</sub> from an urban surface, pollutant (tracer) dispersion and radiation properties with respect to satellite retrieval algorithms.
- To combine full-scale observations with numerical and physical modeling in order to optimally use the advantages of those three basic approaches for the investigation of atmospheric processes. Thus not only numerical modeling studies were advanced in parallel to the observations, but also a wind tunnel model was constructed.

BUBBLE was probably one of the longest and most detailed urban boundary layer programs. Preliminary data analysis has shown the potential and richness of this data set as well as the value it will have to further pursue the work of devising appropriate turbulence exchange parameterizations, be it for numerical models (including operational weather forecast models) or for air pollution dispersion models. The data set can be used to study basic characteristics of urban climate (Christen and Vogt, 2004) including comparisons to other city environments. Also it will help to devise recommendations on the use or estimation of urban meteorological parameters for simple models (e.g. Christen and Rotach, 2004). Apart from giving a quite detailed overview on the activities within BUBBLE the present paper also serves as tool to disseminate the sources of further information that can be obtained on this project. One of the most important resources is the project's web site (<http://www.unibas.ch/geo/mcr/Projects/BUBBLE/>), where information, pictures, publications, detailed instrument information and addresses can be found. It is hoped that BUBBLE data and research will widely be used by the urban boundary layer community, for model evaluation and process studies.

#### Acknowledgements

BUBBLE was made possible by a large number of grants and resources from many institutions and individuals. The core project was financed by the Swiss Federal Office for Education and Science (Grant C00.0068). Additional support for the tracer experiments and the wind tunnel study was provided through an ETH grant (TH 35/02-1). The involvement of the Bulgarian project partner was partly supported through an Institute Partnership financed by the Swiss National Science Foundation (grant 7IP 065650.01) and the analysis of the dispersion data was supported by NATO Linkage Grant (EST-CLG-979863). The analysis of the satellite data was supported by the Swiss National Science Foundation grant No. 2100-067964. Funding from the Canadian Foundation of Climate and Atmospheric Science (GR-022), from Natural Science and Engineering Research Council of Canada, as well as internal funding of Risø National Laboratory (DK), The University of Hamburg (D), The University of Western Ontario (CA), TU Dresden (D), The National University of Singapore, Indiana University (USA) and The University of Padova (I) made the participation and contributions of many of the BUBBLE PIs possible.

We are grateful to many individuals and institutions who have either helped to make BUBBLE possible by letting us

use their property to set up instrumentation or have contributed to constructing infrastructure, setting up sites or helping with the tracer releases. Special thanks go to the Luftthygieneamt beider Basel, METEK GmbH, UMEG Karlsruhe and Forschungszentrum Karlsruhe, Indiana University and the University of Padova for providing pollution data or meteorological instruments for use within BUBBLE.

Thanks to the staff at the University of Basel for their support, Marianne Caroni, Heidi Strohm (laboratory), Günter Bing (IT), Paul Müller (workshop), Josette Pfefferli-Stocky (administration) and also to the engineers of ETH Zurich (Karl Schrott and Hansjürg Frei) for many impossible solutions.

#### References

- Allwine JK, Shinn JH, Streit GE, Clawson KL, Brown M (2002) Overview of URBAN 2000. *Bull Amer Meteor Soc* 83: 521–536
- Aniello C, Morgan K, Busbey A, Newland L (1995) Mapping micro-urban heat islands using Landsat TM and a GIS. *Computers and Geosciences* 21: 965–969
- Argentini S, Mastrantonio G, Lena F (1999) Case studies of the wintertime convective boundary-layer structure in the urban area of Milan, Italy. *Bound-Layer Meteorol* 93: 253–267
- Arritt RW, Young GS (1990) Elevated stable layers generated by mesoscale boundary-layer dynamics over complex terrain. *Proceedings, Fifth Conference on Mountain Meteorology. American Meteorological Society*, 114–117
- Batchvarova E (2003) Progress in urban dispersion and air quality studies. *Preprints 5<sup>th</sup> Int Conf Urban Climate*, 1–5 September 2003, Lodz, PL
- Batchvarova E, Gryning SE (2004) Advances in the modeling of meteorology in urban areas for environmental applications. *NATO Advanced Research Workshop: Advances in air pollution modelling for environmental security, Borovetz (BG)*, 8–12 May 2004
- Batchvarova E, Gryning SE (2005) Progress in urban dispersion studies. *Theor Appl Climatol* (accepted)
- Cenedese A, Cosemans G, Erbrink H, Stübi R (1998) Vertical profiles of wind, temperature and turbulence. In: *Harmonisation of the pre-processing of meteorological data for atmospheric dispersion models COST action 710. Final report Office for Official Publications of the European Communities*
- Christen A, Vogt R (2004) Energy and radiation balance of a Central European City. *Int J Climatol* 24: 1395–1421
- Christen A, Rotach MW (2004) Estimating wind speed at an urban reference height. *Fifth Symposium on the Urban Environment (AMS), Vancouver, Canada*, 23–28 August 2004
- Christen A, Vogt R, Rotach MW (2003a) Profile measurements of selected turbulence parameters over different urban surfaces. *Preprints 4th International Conference on Urban Air Quality, Prague, March 25–27 2003*: 408–411
- Christen A, Bernhofer C, Parlow E, Rotach MW, Vogt R (2003b) Partitioning of turbulent fluxes over different

- urban surfaces. Proceedings Fifth International Conference on Urban Climate, September 1–5 2003, Lodz, Poland, Vol 1: 285–288
- Clappier A, Perrochet P, Martilli A, Muller F, Kruger BC (1996) A new non-hydrostatic mesoscale model using a CVF (control volume finite element) discretisation technique. In: Borrell PM et al (eds) Proceedings EUROTRAC Symposium 96, Comp Mech Publ, Southampton: 527–231
- Clarke CF, Ching JKS, Godowich JM (1982) A study of turbulence in an urban environment. EPA technical report, EPA 600-S3-82-062
- Craig KJ, Bornstein RD (2002) Urbanization of numerical mesoscale models. In: Rotach MW, Fisher B, Piringner M (eds) Workshop on urban boundary layer parameterisations. EUR 20355, (ISBN: 92-894-4143-7), 119: 17–30
- De Bruin HAR, Meijninger WML, Smedman AS, Magnusson M (2002) Displaced-beam small aperture scintillometer test Part 1: The Wintex data set. Bound-Layer Meteor 105: 129–148
- De Bruin HAR, Van den Hurk JJM, Kohsiek W (1995) The scintillation method tested over a dry vineyard area. Bound-Layer Meteor 76: 25–40
- De Haan P, Rotach MW, Werfeli M (2001) Modification of an operational dispersion model for urban applications. J Appl Meteor 40(5): 864–879
- Doran JC, Fast JD, Horel J (2002) The VTMX 2000 Campaign. Bull Amer Meteor Soc 83: 537–551
- Dousset B, Kermadi S (2003) Satellites observation over the Marseille-Berre Area during the Ubl/Clu- Escompte experiment. Proceedings Fifth International Conference on Urban Climate, September 1–5 2003, Lodz, Poland Vol 2: 319–322
- Dousset B, Gourmelon F (2003) Satellite multi-sensor data analysis of urban surface temperatures and landcover. ISPRS Journal of Photogrammetry & Remote Sensing 58: 43–54
- Dupont E, Menut L, Carissimo B, Pelon J, Flamant PH (1997) Comparison between the atmospheric boundary Layer on Paris and its rural suburbs during the ECLAP experiment. Atmos Environ 33: 979–994
- Ecklund WL, Carter DA, Baisley BB (1988) A UHF wind profiler for the boundary layer, brief description and initial results. J Atmos Oceanic Technol 5: 432–441
- Fairey P, Kalaghchy S (1982) Evaluation of thermocouple installation and mounting techniques for surface temperature measurement in dynamic environments. In: Hayes J, Winn CB (eds) Seventh Nat Passive Solar Conference, Amer Solar Energy Soc Inc
- Fedderson B, Leitl B, Rotach MW, Schatzmann M (2003) Wind tunnel investigation of the spatial variability of turbulence characteristics in the urban area of Basel City, Switzerland. Proceedings PHYSMOD2003, September 3–5, 2003, Prato, Italy, Firenze University Press: 23–25
- Fedderson B, Leitl B, Rotach MW, Schatzmann M (2004) Wind tunnel modeling of urban turbulence and dispersion over the City of Basel (Switzerland) within the BUBBLE project. Fifth Symposium on the Urban Environment (AMS), Vancouver, Canada, 23–28 August 2004
- Fisher BEA, Kukkonen J, Schatzmann M (2002) Meteorology applied to urban air pollution problems COST 715. Int J Environment and Pollution, 16: 560–569
- Frioud M, Mitev V, Matthey R, Häberli Ch, Richner H, Werner R, Vogt S (2003) Elevated aerosol stratification above the Rhine Valley under strong anticyclonic conditions. Atmos Environ 37: 1785–1797
- Godovich JM (1986) Characteristics of vertical turbulence velocities in the urban convective boundary layer. Bound-Layer Meteor 35: 387–407
- Grimmond CSB, Oke TR (1999) Aerodynamic properties of urban areas derived, from analysis of surface form. J Appl Meteorol 38(9): 1262–1292
- Gryning SE, Batchvarova E, Rotach MW, Christen A, Vogt R (2003) Roof level urban tracer experiment: measurements and modeling. Preprints 26 NATO/CCMS international technical meeting on air pollution modeling and its application, 26–30 May 2003, Istanbul, Turkey
- Gryning SE, Batchvarova E (2004) Advances in urban dispersion modelling. NATO advanced research workshop: Advances in air pollution modelling for environmental security, Borovetz (BG), 8–12 May 2004
- Gryning S-E, Batchvarova E, Rotach MW, Christen A, Vogt R (2004) Roof-level SF6 tracer experiments in the city of Basel. In: press Zürcher Klimatologische Schriften 91 pp (available from IAC-ETH – see authors address)
- Joffre SA (2002) COST cooperation in meteorology. WMO Bulletin 51: 150–155
- Kaimal JC, Finnigan JJ (1994) Atmospheric boundary layer flows. Oxford University Press, 289 pp
- Kanda M, Moriwaki R, Roth M, Oke TR (2002) Area-averaged sensible heat flux and a new method to determine zero-plane displacement length over an urban surface using scintillometry. Bound-Layer Meteor 105: 177–193
- Kastner-Klein P, Rotach MW (2004) Mean flow and turbulence characteristics in an urban roughness sublayer. Bound-Layer Meteor 111: 55–84
- Lagouarde J-P, Irvine MR, Bonneford J-M, Grimmond CSB, Long N, Oke TR, Salmond JA, Offerle B (2002) Sensible heat flux estimated over the city of Marseille, using a LAS Scintillometer. Preprints 4th Symposium on the Urban Environment American Meteorological Society, Norfolk, VA: 215–216
- Leitl B (2000) Validation data for microscale dispersion modelling. EUROTRAC Newsletter 22: 28–32
- Leone JM, Walker H, Leach MJ, Chin HS, Sugiyama G (2002) Urban effects in numerical models and evaluation with field experiment data: Part I: Sensitivity to urban characterization. Preprints 4th Symposium on the Urban Environment, 20–24 May 2002 in Norfolk, VA: 37–38
- Martilli A, Clappier A, Rotach MW (2002) An urban surface exchange parameterisation for mesoscale models. Bound-Layer Meteor 104: 261–304
- Martilli A, Roulet YA, Jeunier M, Kirchner F, Rotach MW, Clappier A (2003) On the impact of urban surface exchange parameterisations on air quality simulations: the Athens case. Atmos Environ 37: 4217–4231
- Martucci G, Mitev V, Matthey R, Srivastava MK (2003) Remote-Controlled automatic backscatter lidar for PBL

- and troposphere measurements: Description and first results. SPIE International Symposium – Remote Sensing Europe, Conference 5235 – Remote Sensing of Clouds and the Atmosphere VIII, 8–12 September 2003, Barcelona, Spain, paper No 5235-92
- Mestayer PG, Durand P, Augustin P, Bastin S, Bonnefond J-M, Bénech B, Campistron B, Coppalle A, Delbarre H, Dousset B, Drobinski P, Druilhet A, Fréjafon E, Grimmond CSB, Groleau D, Irvine M, Kergomard C, Kermadi S, Lagouarde J-P, Lemonsu A, Lohou F, Long N, Masson V, Moppert C, Noilhan J, Offerle B, Oke TR, Pigeon G, Puygrenier V, Rosant J-M, Saïd F, Salmond J, Talbaut M, Voogt JA (2004) The urban boundary layer field experiment over Marseille UBL/CLU-ESCOMPTE: Experimental set-up and first results. *Bound-Layer Meteorol* (accepted)
- Munier K, Burger H (2001) Analysis of land use data and surface temperatures derived from satellite data for the area of Berlin. In: Jürgens C (ed) *Remote sensing of urban areas/Fernerkundung in urbanen Räumen Regensburg* ISBN 3-88246-222-1: 206–221
- Nichol JE (1998) Visualisation of urban surface temperatures derived from satellite images. *Int J Remote Sensing* 19: 1639–1649
- Nunez M, Oke TR (1976) Long-wave radiative flux divergence and nocturnal cooling of the urban atmosphere II – Within an urban canyon. *Bound-Layer Meteorol* 10: 121–135
- Oke TR (1987) *Boundary layer climates*, 2nd edn. London: Routledge, 435 pp
- Olesen HR, Løfstrøm R, Berkowicz R, Jensen AB (1992) An improved dispersion model for regulatory use: The OML model. In: van Dop H, Kallos G (eds) *Air pollution and its applications IX*. New York: Plenum Press, pp 29–38
- Parlow E (1998) Analyse von Stadtklima mit Methoden der Fernerkundung. *Geographische Rundschau* 50: 89–93
- Parlow E (1999) Remotely sensed heat fluxes of urban areas. In: De Dear RJ, Kalma JD (eds) *Biometeorology and urban climatology at the turn of the millennium: Selected Papers from the Conference ICB-ICUC99*, Sydney: 523–528
- Parlow E (2003) The urban heat budget derived from satellite data. *Geographica Helvetica* 2: 99–111
- Pascheke F, Leidl B, Schatzmann M (2001) Results from recent observations in an urban boundary layer. In: Rotach MW, Fisher B, Piringer M (eds) *Workshop on urban boundary layer parameterisations*, EUR 20355, (ISBN: 92-894-4143-7), 119 pp: 71–83
- Piringer M (ed) (2001) *Surface energy balance in urban areas. Extended abstracts of a COST 715 expert meeting*. Antwerp, April 12 2000, EUR 19447, (ISBN: 92-984-1413-8), 103 pp
- Piringer M, Kukkonen J (eds) (2002) *Mixing height and inversions in urban areas. Proceedings of the workshop 3 and 4 October 2001*, Toulouse, France, (ISBN: 92-984-4214-X), 113 pp
- Price J-C (1983) Estimating surface temperatures from satellite thermal infrared data—a simple formulation for the atmospheric effect. *Remote Sensing Environm* 13: 353–361
- Raupach MR, Antonia RA, Rajagopalan S (1991) Rough-wall turbulent boundary layers. *Appl Mech Rev* 44: 1–25
- Rotach MW (1993) Turbulence close to a rough urban surface Part II: Variances and gradients. *Bound-Layer Meteorol* 66: 75–92
- Rotach MW (1999) On the influence of the urban roughness sublayer on turbulence and dispersion. *Atmos Environ* 33: 4001–4008
- Rotach MW (2001) Simulation of urban-scale dispersion using a Lagrangian stochastic dispersion model. *Bound-Layer Meteorol* 99: 379–410
- Rotach MW, Fisher B, Piringer M (2002) COST 715 Workshop on urban boundary layer parameterizations. *Bull Amer Meteor Soc* 83(10): 1501–1504
- Rotach MW, Fisher B, Piringer M (eds) (2003a) *Workshop on urban boundary layer parameterisations*, EUR 20355, (ISBN: 92-894-4143-7), 119 pp
- Rotach MW, Gryning SE, Batchvarova E, Christen A, Vogt R (2004) Pollutant dispersion close to an urban surface – the BUBBLE tracer experiment. *Meteorol Atmos Phys* 87: 39–58
- Rotach MW, Christen A, Vogt R (2003b) Profiles of turbulence statistics in the urban roughness sublayer with special emphasis to dispersion modeling. *Proceedings Fifth International Conference on Urban Climate*, September 1–5 2003, Lodz, Poland, Vol 1: 309–312
- Roth M (2000) Review of atmospheric turbulence over cities. *Quart J Roy Meteor Soc* 126: 941–990
- Roth M, Salmond J, Satyanarayana ANV, Christen A, Vogt R, Oke TR (2003) Turbulence characteristics, similarity and CO<sub>2</sub> (CO) Spectra over an urban canyon. *Proceedings Fifth International Conference on Urban Climate*, September 1–5 2003, Lodz, Poland, Vol 1: 313–315
- Roulet Y-A (2004) *Validation and application of an urban turbulence parameterization scheme for mesoscale atmospheric models*. PhD thesis Ecole Polytechnique Federal Lausanne (EPFL), 202 pp
- Roulet Y-A, Martilli A, Rotach MW, Clappier A (2003) Modeling of urban effects over the city of Basel (Switzerland) as a part of the BUBBLE project. *Proceedings Fifth International Conference on Urban Climate*, September 1–5 2003, Lodz, Poland, Vol 1: 369–372
- Roulet Y-A, Martilli A, Rotach MW, Clappier A (2004) Validation of an urban surface exchange parameterization for mesoscale models – 1D case in a street canyon. *J Appl Meteorol* (in press)
- Ruffieux D (1999) Use of a wind profiler in a planetary boundary layer experiment. *Analysis* 27(4): 18–21
- Ruffieux D, Tharin N, Berger H (2002) Use of a low-tropospheric wind profiler within an urban environment. *Proceedings Instruments and Observing Methods TECO-2002*, Bratislava (SL), 23–25 September, 2002 WMO Report No 25, WMO/TD-No 1123
- Salmond JA, Roth M, Oke TR, Satyanarayana ANV, Christen A, Vogt R (2003) Comparison of turbulent fluxes from roof top versus street canyon locations using

- scintillometers and eddy covariance techniques. Proceedings Fifth International Conference on Urban Climate, September 1–5 2003, Lodz, Poland, Vol 1: 317–320
- Schatzmann M, Rafailidis S, Duijm NJ (1999) Wind tunnel experiments. In: Fenger J, Hertel O, Palmgren F (eds) Urban air pollution – European aspects. Elsevier Sci Publ, ISBN 0-7923-5502-4: 261–276
- Schatzmann M, Brechler J, Fisher B (eds) (2001) Preparation of meteorological input data for urban site studies. EUR 194665, (ISBN: 92-894-0923-1), 101 pp
- Schmid HP (1994) Source areas for scalars and scalar fluxes. *Bound-Layer Meteor* 67: 293–318
- Tennekes H, Lumley JJ (1972) A first course in turbulence. Cambridge: MIT Press, 300 pp
- Vogt R, Christen A, Rotach MW, Roth M, Satyanarayana ANV (2003) Fluxes and profiles of CO<sub>2</sub> in the urban roughness sublayer. Proceedings Fifth International Conference on Urban Climate, September 1–5 2003, Lodz, Poland, Vol 1: 321–324
- Voogt JA, Oke TR (1991) Validation of an urban canyon model for nocturnal long-wave radiative fluxes. *Bound-Layer Meteor* 54: 347–361
- Weber BL, Wuertz DB, Welsh DC, McPeck R (1993) Quality controls for profiler measurements of winds and RASS temperatures. *J Atmos Oceanic Technol* 10(4): 452–464
- Weiss A, Hennes M, Rotach MW (2001) Derivation of refractive index- and temperature gradients from optical scintillometry for the correction of atmospheric induced problems in highly precise geodetic measurements. *Surv Geophys* 22: 589–596
- White AB (1993) Mixing depth detection using 915-MHz radar reflectivity data. Preprints 8th Symp Observations and Instrumentation. Amer Meteor Soc, Boston, pp 248–250
- Wilczak JM, Strauch RG, Ralph FM, Weber BL, Merritt DA, Jordan JR, Wolfe DE, Lewis LK, Wuertz DB, Gaynor JE, McLaughlin SA, Rogers RR, Riddle AC, Dye TS (1995) Contamination of wind profiler data by migrating birds: characteristics of corrupted data and potential solutions. *J Atmos Oceanic Technol* 12(3): 449–467

Authors' addresses: Mathias W. Rotach (e-mail: mathias.rotach@meteoswiss.ch), Dominique Ruffieux, Swiss Federal Office for Meteorology and Climatology, MeteoSwiss, Krähbühlstrasse 58, P.O. Box 514, 8044 Zürich, Switzerland; Roland Vogt, Andreas Christen, Eberhard Parlow, University of Basel, Institute for Meteorology, Climatology and Remote Sensing, Basel, Switzerland; Christian Bernhofer, University of Dresden, Germany; Ekaterina Batchvarova, Bulgarian National Institute of Meteorology and Hydrology, Bulgaria; Alain Clappier, Yves-Alain Roulet, Swiss Federal Institute of Technology, Laboratory of Air and Soil Pollution, LPAS-EPFL, Switzerland; Berend Feddersen, Michael Schatzmann, University of Hamburg, Meteorology Department, Germany; Sven-Erik Gryning, Risø National Laboratory, Department for Wind Energy, Denmark; Helmut Mayer, University of Freiburg, Meteorological Institute, Germany; Giovanni Martucci, Valentin Mitev, Observatory of Neuchâtel, Switzerland; Timothy R. Oke, The University of British Columbia, Geography Department, Canada; Matthias Roth, The National University of Singapore, Geography Department, Singapore; Jennifer A. Salmond, Birmingham University, Geography Department, England; James A. Voogt, University of Western Ontario, Geography Department, Canada.